# Progress in Materials Science

An International Review Journal

## Editors

J.W. CHRISTIAN
Department of Metallurgy,
University of Oxford, Oxford OX1 3PH, U.K.

P. HAASEN
Institut für Metallphysik,
Universität Göttingen, D3400 Göttingen, F.R.G.

T.B. MASSALSKI
Department of Met. Eng. & Materials Science
Carnegie-Mellon University, Pittsburgh, PA 15213, U.S.A.

**Subscription Rates 1986**

Annual Subscription: $145.00 post free

Two-year Subscription: $275.50 post free

*Specially Reduced Rates to Individuals*: Any individual whose institution takes out a library subscription may purchase a second or additional subscription for personal use at a much reduced rate of U.S. $50.00 per annum.

Single back volumes and parts are available. *Subscription enquiries from customers in North America should be sent to* Pergamon Journals, Inc., Maxwell House, Fairview Park, Elmsford, NY 10523, U.S.A., *and for the remainder of the World to* Subscription Fulfillment Manager, Pergamon Journals Ltd., Headington Hill Hall, Oxford OX3 0BW, England.

At the end of the volume the subscriber will receive, free, the subject index and an attractive and durable magazine binder especially designed for *Progress in Materials Science*.

Subscribers in the U.S. and Canada receive their copies by air, post free.



*The Item-Fee Code for this publication is*: 0079-6425/86 $0.00 + .50

Library of Congress Catalog Card No. 76-26739.

## Publishing/Advertising Offices

Pergamon Journals Ltd.,
Headington Hill Hall,
Oxford OX3 0BW, England

Pergamon Journals Inc.,
Maxwell House,
Fairview Park, Elmsford,
New York 10523, U.S.A.

## Microform Subscriptions and Back Issues

Back issues of all previously published volumes are available in the regular editions and on microfilm and microfiche. Current subscriptions are available on microfiche simultaneously with the paper edition and on microfilm on completion of the annual index at the end of the subscription year.

ress in Materials Science Vol. 30, pp. 1 to 37, 1986
ed in Great Britain. 

0079-6425/86 $0.00 + .50


# KINETICS OF ISOTHERMAL MARTENSITIC TRANSFORMATION

*Naresh N. Thadhani*† *and Marc A. Meyers*‡

†Division of Engineering and Applied Science/Materials Science, California Institute of Technology, Pasadena, California, U.S.A.

‡Center for Explosives Technology Research and Department of Metallurgical and Materials Engineering, New Mexico Institute of Mining and Technology, Socorro, New Mexico, U.S.A.

## CONTENTS



## NOMENCLATURE

| | |
|---|---|
| $f_s$ | Austenite-to-martensite reaction start temperature |
| | Gamma austenite (fcc) |
| ′ | Alpha martensite (bcc) |
| | Number of embryos initially present per unit volume |
| $_c$ | Number of embryos per unit volume consumed to martensite plates |
| | Total number of embryos per unit volume existing at time $t$. |
| | Autocatalytic factor or number of autocatalytically produced sites |
| | Fraction of martensite formed |
| $W_a$ | Activation energy for nucleation of martensite |
| | Lattice vibration frequency per second |
| $t$ | Thickness-to-diameter ratio for martensite plates |
| | Average volume per grain of austenite |
| | Fraction of grain volume transformed to martensite |
| | Number of martensite plates formed within austenite grains |
| | Mean volume per martensite plate |
| | Mean reciprocal of martensite plate lengths as intersected by a random plane |
| $N_A$ | Number of martensite plates per unit area of random cross-section |
| | Volume of martensite plate |



P.M.S. 30/1—A

| | |
|---|---|
| $n^*(Q)\mathrm{d}Q$ | Number of nucleation sites per unit volume having activation energies between $Q$ and $\mathrm{d}Q$ |
| $\chi$ | Fraction of particle transformed to martensite |
| $V_p$ | Volume of particle |
| $M_B$ | Temperature at which martensite transformation starts with a burst |
| $S_v$ | Density of internal surface of martensite plates |
| $V_v$ | Volume fraction of martensite transformed in a burst |
| $G_g$ | Fraction of material in grains partially transformed to martensite |
| $\Delta G$ | Thermodynamic free energy for the formation of one mole of martensite |
| $\sigma$ | Interfacial energy |
| $A$ | Strain energy factor |
| $r_e$ | Martensite embryo radius (potency) |
| $\bar{v}(\alpha')$ | Average volume per martensitic unit |
| $\bar{v}(sb)$ | Average volume of a shear band |
| $n$ | Number of intersections of planar features |
| $P_r$ | Probability of embryo formation on intersection |
| $\alpha$ | Strain-independent constant |
| $\epsilon$ | Plastic strain |
| $R$ | Ratio between initial nucleation sites and autocatalytically produced sites |
| $z$ | Parameter related to probability of nucleation and to average volume of martensite plates |

## 1. INTRODUCTION

While the crystallography of martensite was established in the 1930s, it was only in 1950 that Kurdjumov and Maksimova[1] first observed that the amount of martensite could increase with time at a constant temperature. This behavior of martensitic transformation has been named "isothermal". To the authors' knowledge, Fisher *et al.*[2,3] were the first to apply the theory of nucleation and growth to martensitic transformation. They treated it along the "classical" path, in which the structure of embryo is the same as that of the martensite, and a nucleation barrier has to be overcome. Upon cooling, Fisher *et al.*[3] stated that nucleation took place independent of thermal motion. Hence, they termed the martensite forming as a function of temperature *athermal*, while they reserved the term *isothermal* for the martensite requiring "thermal nucleation".

Isothermal martensitic transformation was explained[1] as a direct result of extending the classical theory of fluctuational nucleation to martensitic transformations. Today there are numerous examples available that rule out the athermal mode (fraction transformed independent of time) of transformation kinetics as the necessary manifestation of a martensitic reaction. Generally, the isothermal reaction is observed to occur below the $M_s$, but there are some examples known in which martensite can form isothermally above the $M_s$. In many martensitic systems, the isothermal component is either obscured by the predominant athermal behavior or is operative in so small a scale in time that it is virtually impossible to detect the characteristics of the very beginning of the phenomenon.

The isothermal reaction propagates by the nucleation of new plates, rather than by the growth of existing ones. Complete growth occurs within a small fraction of a second. Forster and Scheil[4–6] were the early pioneers to measure the rate of propagation of martensite. They recorded the sonic characteristics of the transformation process on a cardiograph and observed that individual martensite plates form in less than $10^{-4}$ s. In 1953, Bunshah and Mehl[7] estimated that the rate of growth of martensite plates in Fe–Ni–C alloys was 1100 m/s, implying that such growth rates are of the order of one-third the velocity of sound propagating in metals. In a recent investigation, Meyers,[8] based on martensitic transformations induced by a tensile stress pulse formed by the reflection of a shock wave at a free surface, estimated the nucleation time for martensite to be around 55 ns. Recently, several techniques have been developed based on kinephotometry,[9] involving reflectivity changes

due to surface relief, and emission of acoustic signals associated with bursting.[10–14] They have confirmed that the martensitic transformation occurs in time durations of about 0.1 $\mu$s. Such rapid growth is normal for martensitic reactions in ferrous alloys.

## 2. Qualitative Kinetic Classification of Martensitic Transformations in Ferrous Alloys

It is possible to divide a wide variety of reaction kinetics observed in martensitic transformations in ferrous alloys, into two distinct classes: athermal and isothermal. While the fraction of the transformed phase increases with time at a specific temperature, for the isothermal case, it is constant for the athermal case. Different classification schemes based on the observed kinetic behavior and stabilization have been proposed.

(a) Raghavan and Entwisle[15]

(i) "Athermal" transformation: here the reaction progresses with the decrease in temperature, e.g. in carbon and low alloy steels.

(ii) "Burst" transformation: here the reaction starts with an abrupt burst in alloys having transformation ranges at sub-zero temperatures, e.g. in Fe–Ni and Fe–Ni–C alloys.

(iii) "Completely isothermal" transformation: this behavior is exhibited in alloys below room temperature, such that the reaction progresses with increase in time at a constant temperature, e.g. Fe–Ni–Mn and Fe–Ni–Cr alloys.

(b) Magee[16]

(i) "Athermal" behavior: associated with dynamic stabilization, e.g. in Fe–1.1% C, the transformation occurs because of the presence of interstitials (carbon or nitrogen).

(ii) "Isothermal" behavior: here both the burst and completely isothermal behavior are grouped together, the common feature between them being the absence of concurrent stabilization, e.g. bursting in Fe–31% Ni and isothermal transformation in Fe–24% Ni–3% Mn alloys.

(c) Raghavan and Cohen[17]

They redefined the sub-classification for transformation behavior at sub-zero temperatures and grouped them into two categories:

(i) "Completely isothermal" transformation to lenticular martensite occurring in an Fe–29% Ni alloy within a narrow temperature range and in which the isothermal characteristics are observable from the very start of the transformation.

(ii) "Anisothermal" transformation occurs when the same alloy is further cooled to lower temperature during which bursting with an audible click occurs with a substantial amount of martensite forming within $\mu s$, because of autocatalysis.

The athermal reaction is thought to have close ties with the isothermal one. There have been proposals,[1,18] that athermal martensite is in fact an ultra-fast isothermal martensite. The distinction between the two is believed to be purely empirical.

(iii) Guimarães[19] added, to the classification of Raghavan and Entwisle,[15] a fourth class of transformations: the mechanically-induced martensite. This martensite forms as the alloy is mechanically deformed. The fraction transformed can be

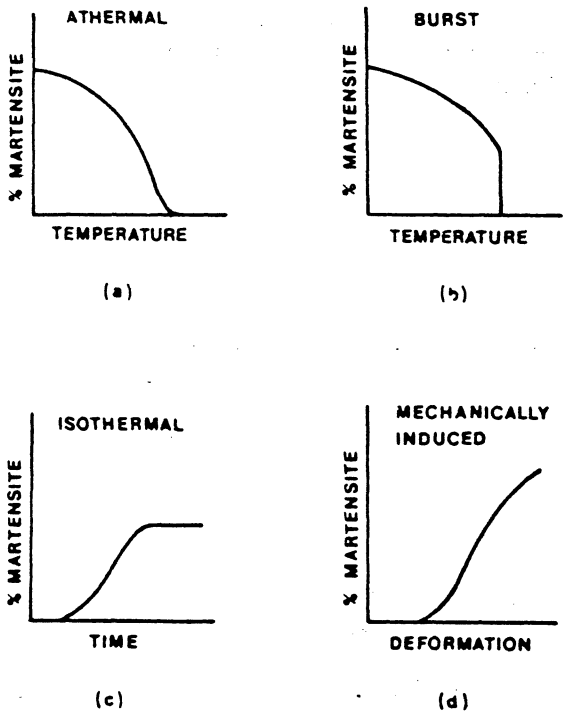


FIG. 1. Schematic representation of the four types of kinetic background behavior observed in martensitic transformations: (a) athermal; (b) burst; (c) isothermal; (d) mechanically-induced (Fig. 2 in Ref. 19).

expressed as a function of strain. Section 8 presents a discussion on the effect of imposed plastic strain on the fraction transformed.

Figure 1 shows schematically the four types of transformation responses observed for ferrous alloys. For athermal martensite [Fig. 1(a)], the fraction transformed increases continuously with a decrease in temperature. For "burst" martensite [Fig. 1(b)] there is initially a discontinuity; below that temperature, the fraction transformed behaves in a manner similar to the athermal martensite. Isothermal martensite shows an increase in fraction transformed with time [Fig. 1(c)]. The gradual increase in fraction transformed can either precede or follow a "burst". The mechanically induced martensite [Fig. 1(d)] shows an increase with plastic strain.

## 3. REVIEW OF EXPERIMENTS ON ISOTHERMAL KINETICS

Most martensitic transformations, particularly in ferrous alloys, have been studied athermally as a function of decreasing temperature. However, the best quantitative understanding on the kinetics of the reaction can be obtained from isothermal transformations which permit nucleation rates and transformation rates to be determined experimentally. These experiments have shown that at each reaction temperature, the transformation starts in the virgin austenite and proceeds as a function of time. The transformation exhibits a C-curve behavior, typical of isothermal reactions. The isothermal formation of martensite is

now a well established fact in a number of alloys. A brief review is presented below in chronological order:

(a) Kurdjumov and Maksimova[1] in 1948 and 1950, were the first to report the isothermal formation of martensite in 1.6% C steel, occurring below −100°C. They also observed a C-curve characteristic in another 0.6% C–6% Mn–27% Cu steel and in an Fe–23% Ni–3.4% Mn alloy. The nose temperature (at which the transformation rate was highest) was observed to be around −130°C.

(b) Averbach and Cohen,[20] in 1949, observed that the hardening reaction (martensitic) occurring during the quenching of plain carbon or low carbon alloy tool steels did not stop immediately when room temperature was reached, but rather, the austenite continued to transform although at a slower rate. At that time it was believed that the isothermal formation of martensite was merely a "tailing off" effect, since only a small amount of austenite was transformed.

(c) Das Gupta and Lement,[21] in 1951, observed isothermal behavior in a 0.7% C–15% Cr steel following some athermal transformation occurring in the range of −65 to −196°C.

(d) Machlin and Cohen,[22] in 1951, observed that the transformation in Fe–30% Ni alloys occurred by bursting and about 25% of the austenite transformed during cooling below ambient temperature within the time interval of a single audible click. Later, they also found that the isothermal rate of martensite formation in an Fe–29% Ni alloy[23] was dependent upon the temperature and time of the isothermal hold, the amount of athermal martensite present, and the state of internal and applied stress.

(e) Kulin and Speich,[24] in 1952, studied the isothermal formation of martensite in an austenitic stainless steel (Fe–14.4% Cr–9% Ni) and found that the transformation followed a C-curve behavior with the nose at −30°C. Typical isothermal transformation curves are shown in Fig. 2.

(f) Cech and Hollomon,[25] in 1953, did experiments similar to Kurdjumov and Maksimova on an Fe-23% Ni–3.7% Mn alloy and observed an isothermal behavior (C-curve) between −79° and −196°C, with a maximum at −130°C.

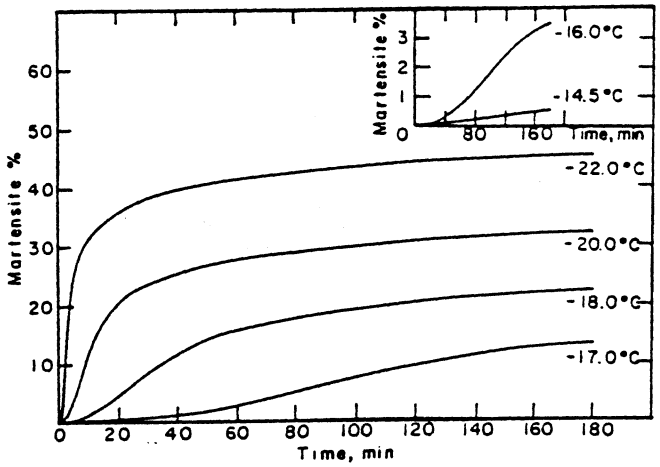


FIG. 2. Typical isothermal transformation curves for Fe–29% Ni–0.2% Mn–0.006% C steel (Fig. 3 in Ref. 17).

(g) Shih *et al.*[26] in 1955, studied isothermal formation of martensite in Fe–Ni–Mn and Fe–Mn–C alloys after completely avoiding any athermal (surface or bulk) martensite. They found that the initial rate of martensite formation was extremely low under these conditions but subsequently increased with the formation of some martensite. This led to the belief that the true initial characteristics of the isothermal reaction can be studied only in the absence of any prior martensite. Later, Entwisle,[18] Pati and Cohen,[27] and the small particle experiments by Cech and Turnbull,[28] and Magee[29] confirmed this important point in several Fe–Ni–Mn alloys. Raghavan and Cohen[17] electroplated several samples of Fe–24% Ni–3% Mn alloy and showed that the transformation rates during the early stages were always slower in the plated specimens than in the unplated ones, as shown in Fig. 3, because of the absence of any surface martensite. Surface martensite[30] is produced because the strain developed by the martensite is relieved more easily on a free surface than in the interior. This surface martensite, on its turn, can stimulate the bulk transformation by spreading inwards from the surface.

(h) Philibert and Crussard[31] and Philibert[32] in 1955 and 1956 respectively, showed that limited amounts of isothermal martensite may form after the regular cooling transformation. In an Fe–29% Ni alloy, holding at any constant temperature gives an isothermal curve, with a slower transformation in the beginning, but increasing with time before falling off (sigmoidal shape). They also showed that in the absence of interstitials the isothermal mode dominates over burst character at higher temperatures. Woodilla *et al.*[33] also showed that interstitial elements like carbon and nitrogen can play an important role in the stabilization phenomenon.

(i) Yeo[34] showed in 1962 that thermal stabilization due to carbon can be avoided in the presence of a strong carbide forming element such as titanium. Subsequently, an Fe–25% Ni alloy can be isothermally transformed to more than 90% martensite.

(j) Raghavan and Entwisle[15] in 1965 studied the isothermal transformation in an Fe–26% Ni–2% Mn alloy and showed that the transformation curves were very sensitive to changes in grain size. Figure 4 shows the transformation curves obtained by them at −78.5°C for different values of the austenitic grain size. The effect of grain size on isothermal transformation kinetics will be dealt with in greater detail in Section 7.

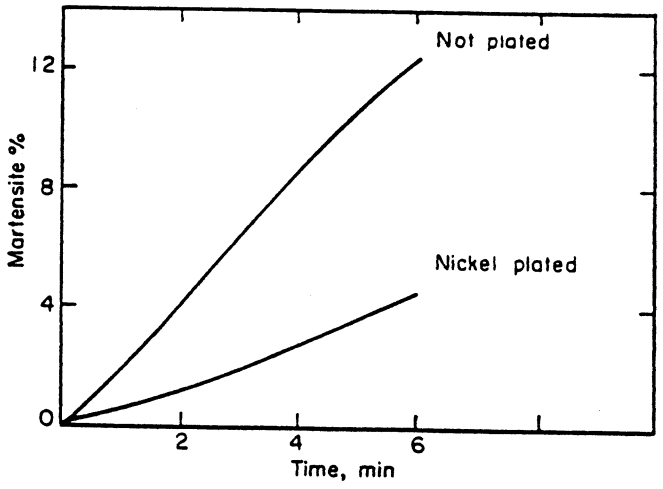


FIG. 3. Effect of nickel plating on isothermal martensitic transformation (Fig. 9 in Ref. 17).

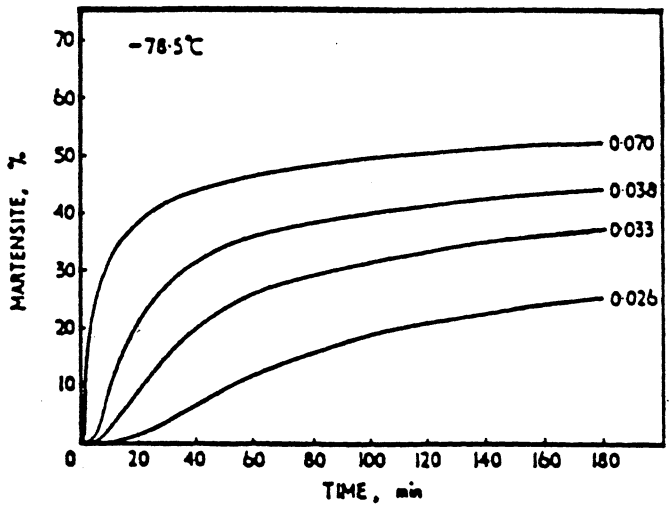


FIG. 4. Transformation curves at −78.5°C for different values of austenitic grain size (Fig. 3 in Ref. 15). Grain sizes in mm are indicated in plot.

(k) Anandaswaroop and Raghavan[35] prequenched an Fe–29% Ni alloy at −95°C before measuring the isothermal nucleation rates upon reheating from the prequenching temperature and found the nose temperature to occur at −70°C.

(l) Pati and Cohen,[27] in 1969, measured the nucleation rates of the isothermal martensitic transformation, using quantitative metallography and electrical resistivity techniques in a series of Fe–23 ~ 25% Ni–2 ~ 3% Mn alloys as a function of austenitic grain size and reaction temperature. They observed a typical C-curve kinetics with the maximum nucleation rate occurring at −125°C. Later (in 1971) they proposed a kinetic model[36] to account for the observed transformed behavior.

(m) Entwisle and Feeney,[37] in 1969, investigated the effect of austenitizing temperature on the martensitic transformation by bursting in Fe–Ni–C alloys with Ni and C ranging between 19–27% and 0.48–0.52% respectively. The magnitude of the burst was a function of the austenitic grain size.

(n) Entwisle,[18] in 1971, surveyed the main features of martensitic transformation kinetics and divided the broad category of reaction kinetics into athermal, burst, completely isothermal and surface transformation. He concluded that there was no practical distinction between athermal and isothermal kinetics and that athermal transformation should in fact be regarded as a rapid isothermal transformation.

(o) Raghavan and Cohen,[17] in 1972, measured the rate of isothermal transformation in Fe-Ni binary alloys containing no prior martensite. Figure 5 shows the transformation curves for an Fe–28.8% Ni alloy, at different reaction temperatures. They observed that the isothermal transformation kinetics were extremely sensitive to the reaction temperature, being barely measurable at −14.5°C and too rapid at −22°C.

(p) Korenko,[38] in 1973, studied the isothermal transformation kinetics in Fe–Ni and Fe–Ni–Mn alloys with the application of a magnetic field. In iron-based alloys the application of a magnetic field induces an additional free energy difference between the parent (paramagnetic) and the product (ferromagnetic) phases. He found that in the Fe–Ni alloys, the isothermal transformation rate increased by raising the magnetic

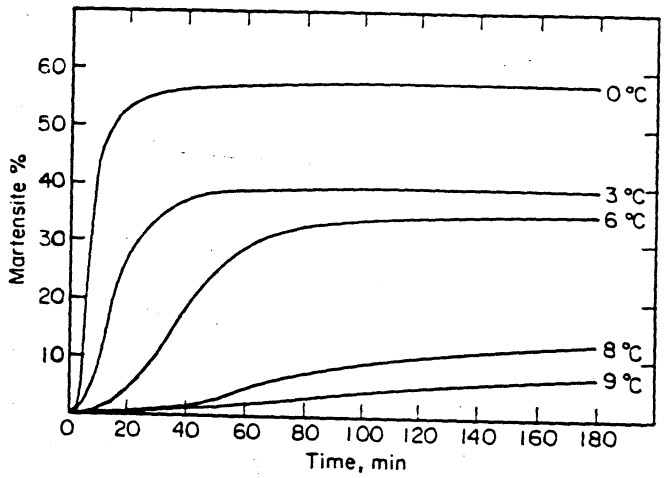


FIG. 5. Transformation curves for Fe–28.8% Ni alloy at different temperatures (Fig. 6 in Ref. 17).

field as well as by lowering the temperature, in either case exhibiting burst characteristics. The Fe–Ni–Mn alloy, on the other hand, exhibited C-curve kinetics only under the application of a magnetic field.

(q) Gupta and Raghavan,[39] in 1975, computed the limiting fraction of martensite at any reaction temperature from experimental isothermal martensitic transformation curves. Their results indicate a strong correlation between the two kinetic modes (athermal and isothermal) and that the isothermal kinetics obeys the empirical relationships known for the athermal mode.

(r) Olson and Cohen[40] proposed a general mechanism for martensite nucleation. They suggested that the growth of embryos in the fault plane was the most likely rate limiting step to account for the observed isothermal as well as athermal kinetics, depending on the parameters controlling the motion of the transformational dislocations.

(s) Garosshen and Galligan,[12] in 1980, monitored the transformation of various Fe–Ni alloys at constant temperatures, by recording the acoustic emission signal associated with the transformation. Their experiments on Fe–Ni alloys showed that there was a time delay in the appearance of a martensitic transformation, as evidenced by an acoustic emission signal. This is consistent with an isothermal process preceding the athermal portion of the reaction and suggests that athermal martensite can exhibit time delays which occur in an isothermal manner.

(t) Moiseyev *et al.*,[14] in 1981, studied the isothermal martensitic transformation in iron and its alloys with different amounts of Ni, using magnetic and dilatation procedures. They observed that in alloys with up to 9% Ni the transformation was too rapid to observe the development of the transformation process at temperatures below the nose of the C-shaped curve. In alloys containing more than 12% Ni the transformation rate first increased reaching a maximum at 430°C, and then falling off to a minimum at 350°C, and finally starting up again with further decrease in temperature.

(u) Kolomytsev *et al.*,[41] in 1981, determined the effect of impact impulse duration at pressures of 10 and 20 GPa on the direct ($\gamma \rightarrow \alpha'$) and reverse ($\alpha' \rightarrow \gamma$) martensitic transformations in an Fe–31.2% Ni alloy. They observed an increase in the amount

of the transformed phase with an increase in the impulse duration. The time required for the formation of $\alpha'$ phase was less than $10^{-7}$ s.

(v) Kajiwara,[42] in 1981, investigated isothermal martensite transformation in Fe–Ni–Mn alloys from a crystallographic viewpoint. He observed that the invariant-plane strain condition on the habit plane was operative from the very early stage of the transformation, in contradiction with Olson and Cohen's model.[40] He also proposed[43,44] that an alternative rate controlling step for isothermal martensite formation was the thermally activated motion of lattice dislocations in austensite to plastically relax the shape strain of martensite, and a small dilatation along the habit plane.

(w) Yang and Wayman[45] observed the simultaneous occurrence of both athermal and isothermal transformation in an Fe–20% Ni–4% Mn alloy with the athermal reaction preceding the isothermal mode. They studied the kinetic characteristics of this alloy using electrical resistance measurements and showed that the formation of isothermal martensite is significantly influenced by formation conditions and prior heat treatment.

(x) Rodrigues *et al.*[46] utilized low temperature dilatometry correlated with internal friction measurements to show that Fe–Ni and Fe–Ni–C alloys exhibit a C-curve isothermal behavior in the 38–200 K temperature range. They also established that quantitative analysis of isothermal martensitic transformation was strongly dependent on experimental conditions and that the internal stresses played an important part in the development of the isothermal reaction.

(y) Thadhani and Meyers,[47,48] by applying tensile stress pulses to an Fe–32% Ni–0.035% C alloy, were able to trigger the formation of martensite at temperatures above $M_s$. By varying the duration of these tensile pulses they obtained varying amounts of transformation. Figure 6 shows their principal results. It is clear that,

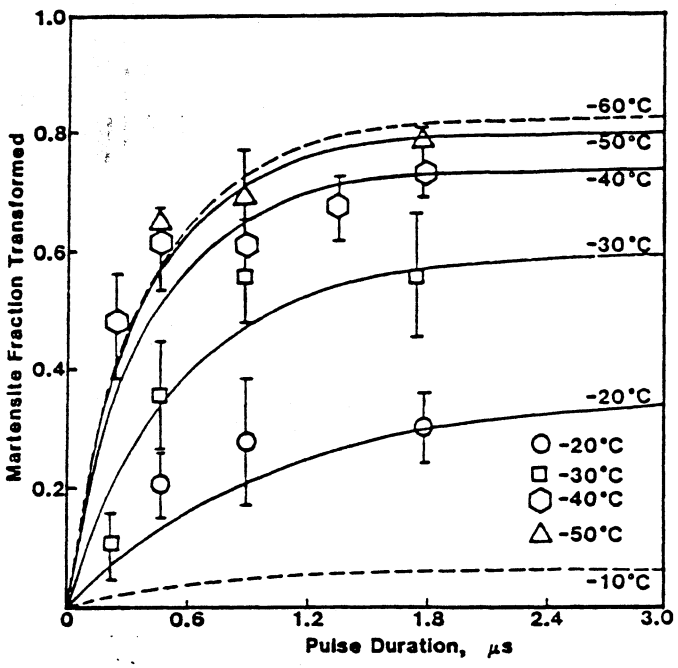


FIG. 6. Fraction transformed as a function of time for Fe–32% Ni–0.035% Ni alloy subjected to tensile stress pulse (Fig.7 in Ref. 48).

within the time window of a $\mu$s, the transformation, considered to be athermal (burst) in this alloy, is indeed isothermal. Thus, these experiments verify the earlier contentions of Magee[16] and Entwisle.[18]

## 4. Quantitative Models for Isothermal Kinetics

Isothermal martensitic transformation kinetics comprises two major effects: an initial increase in the transformation rate followed by a subsequent decrease. The initial increase is attributable to autocatalytic nucleation by which the first martensitic plates produce more nucleation sites than they use (one nucleus giving rise to one plate) or sweep out. Quantitative metallography measurements[27] also support this observation. The subsequent decrease in the transformation rate is because of the partitioning effect during which the austenite is compartmentalized into smaller and smaller packets. As such, the volume fraction of martensite transformed per nucleation event progressively decreases. Several models have been proposed which consider these effects and provide for a quantitative understanding of the isothermal martensitic kinetics. Figure 7 is a schematic representation of nucleation sites being used and produced. The plate will eliminate all embryos contained in its volume (marked by ⊞) and will generate new sites (marked ★). The original nucleation site is also eliminated (⊕).

### 4.1. *Isothermal Kinetic Models*

(i) Raghavan and Entwisle[15] introduced a phenomenological theory, based on the assumption that, upon the formation of a martensite plate, embryos are created in the surrounding austenite matrix. These can be activated thermally and form more martensite plates. If $n_i$ is assumed to be the number of embryos initially present, per unit volume, then in addition to that new embryos are produced autocatalytically in proportion to the volume fraction of martensite formed. At the same time, $N_v$ embryos/cm$^3$ of the alloy are consumed by activation to martensitic plates and so the total number of embryos, $n_t$, existing at time '$t$' per unit volume of the alloy is:

$$n_t = (n_i + pf - N_v)(1 - f) \tag{4.1}$$

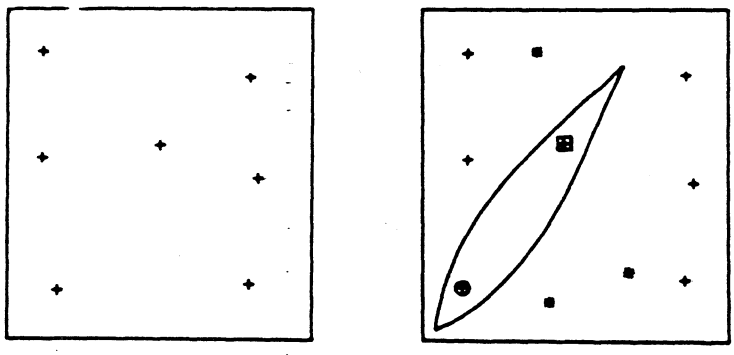

FIG. 7. Schematic representation of autocatalytic formation and sweeping-out of embryos.
+ Original embryos
⊕ Embryo used in nucleation
* Autocatalytically-produced embryo
⊞ embryo swept out

where $p$ is the autocatalytic factor or the number of autocatalytically produced embryos arising due to elastic and plastic strains set up in the surrounding austenite by the martensite plate, and $f$ is the fraction of martensite formed. The first term on the right hand side of eq. (4.1) represents the net number of embryos per unit volume of the alloy potentially available for nucleation at time '$t$'. The second term $(1-f)$ arises because a fraction '$f$' of such embryos is not available since they are swept out by the martensite formed. However, in the early stages of the transformation this term can be disregarded.

If all embryos are assumed to have the same activation energy, $\Delta W_a$, the overall rate of transformation can be expressed as the product of the nucleation rate and the volume fraction transformed per nucleation event. Adopting the partitioning model of Fisher *et al.*[3] Raghavan and Entwisle obtained[15]:

$$\frac{df}{dt} = (n_i + pf - N_v)(1-f)\nu\left[\exp\left(-\frac{\Delta W_a}{RT}\right)\right] \times mq\,(1-f)^{1+1/m} \tag{4.2}$$

where $\nu$ is the lattice vibration frequency ($10^{13}$ per second): $m$ is the thickness-to-length ratio for the martensite plates; and $q$ is the average volume per grain of austenite.

By numerical integration of eq. (4.2) one can compute the percentage of martensite as a function of time. The values of $q$ and $m$ can be obtained from metallographic measurements, leaving two unknowns: $\Delta W_a$ and $p$. These can then be evaluated by curve-fitting the calculated to the experimental results. Figure 8 shows the comparison of the experimental transformation curves with those computed from eq. (4.2) for an Fe–26% Ni–2% Mn alloy transformed at −66°C, having different grain sizes. It can be seen that the agreement is good only up to 8–10% transformation.

(ii) Raghavan[49] based his model on the assumption that martensite plates form uniformly in clusters rather than randomly during the early stages of the transformation. He divided the transformation process into two arbitrary steps: (a) the increase in time of the number of austenite grains where the first plate nucleation takes place; and (b) the process of transformation with time within the austenite grains which already have the first martensite

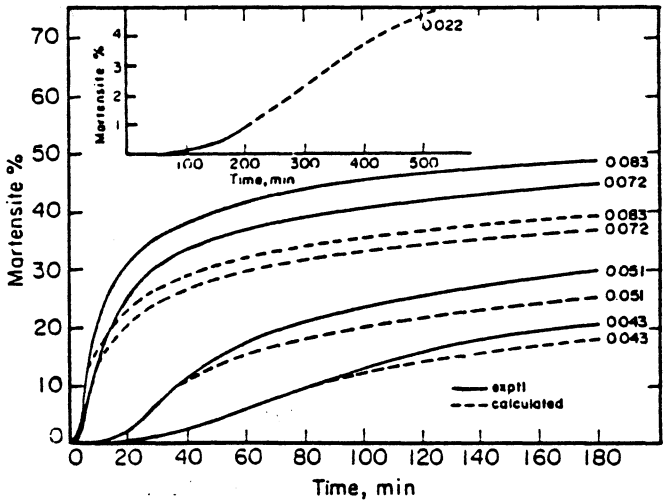


FIG. 8. Experimental and calculated transformation curves for an Fe–26% Ni–2% Mn alloy transformed at −66°C for a range of grain sizes (Fig. 10 in Ref. 15).

plates. This implies that the overall transformation rate is a function of the "spreading-over" as well as the "filling-in" processes which occur simultaneously. Modifying Fisher's partitioning formula, Raghavan expressed the transformation rate as:

$$\frac{df_g}{dt} = (n_i q + qpf_g - P)(1-f)v\left\{\exp\left(-\frac{\Delta W_a}{RT}\right)\right\} m (1-f_g)^{1+1/m} \tag{4.3}$$

where $f_g$ is the fraction of grain volume transformed and $P$ is the number of martensite plates formed within the grains.

Raghavan's model is observed to agree with the experimental transformation curves up to 13% only, as shown in Fig. 9.

(iii) Pati and Cohen[36] showed that the Fisher partitioning formula adopted in the previous models, over estimates the number of martensitic plates required to give a certain fraction of transformation, especially beyond 20% martensite. Hence they introduced experimental data obtained from quantitative metallographic measurements to generate the isothermal transformation curves. They computed the values of the mean volume per martensite plate, $\bar{v}$, for all the plates present in an Fe–24% Ni–3% Mn alloy transformed at various reaction temperatures around $-125$°C. They found that $\bar{v}$ depends not only on the extent of the transformation (partitioning), but also on the reaction temperature as shown in Fig. 10.

Hence, Pati and Cohen incorporated actual measurements in order to avoid any reliance on a partitioning relationship. The number of most potent embryos, $n_t$, existing at any time, per unit volume as given by eq. (4.1) is:

$$n_t = (n_i + pf - N_v)(1-f).$$

Employing Fullman's[50] equation,

$$N_v = \frac{f}{\bar{v}} \tag{4.4}$$

and with eq. (4.1) one obtains:

$$N_t = \left[n_i + f\left(p - \frac{1}{\bar{v}}\right)\right](1-f). \tag{4.5}$$

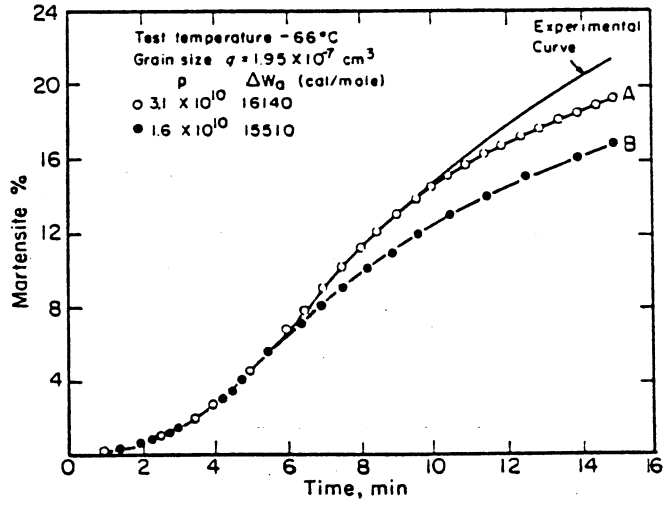


FIG. 9. Comparison of experimental and calculated transformation curves according to Raghavan's model, for an Fe–26% Ni–2% Mn alloy at −66°C (Fig. 3 in Ref. 49).

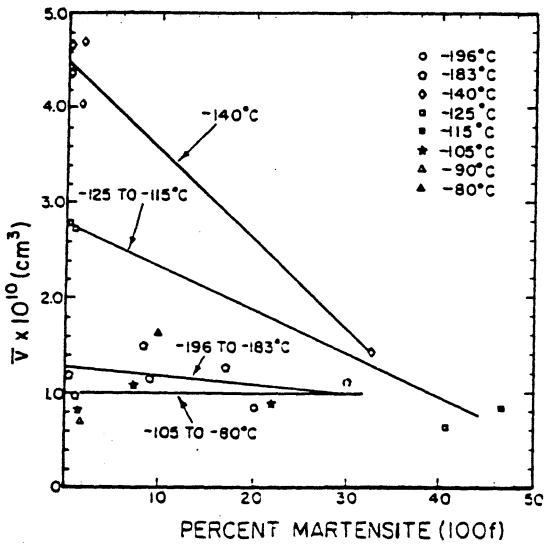


FIG. 10. Variation of the mean volume ($\bar{v}$) per martensite plate as a function of percentage martensite transformed at various temperatures in an Fe–24 Ni–3 Mn alloy (Fig. 1 in Ref. 36).

The rate of activation of such embryos per unit volume or the formation rate of martensite plates can be expressed as:

$$\frac{dN_v}{dt} = \left[n_i + f\left(p - \frac{1}{\bar{v}}\right)\right](1-f)\nu \exp\left(\frac{\Delta W_a}{RT}\right). \tag{4.6}$$

The isothermal transformation rate is given by,

$$\frac{df}{dt} = \left(\frac{dN_v}{dt}\right) V. \tag{4.7}$$

Also from eq. (4.4),

$$\frac{df}{dt} = \frac{d(N_v \cdot \bar{v})}{dt} = \bar{v}\frac{dN_v}{dt} + N_v\frac{d\bar{v}}{dt} = \frac{dN_v}{dt}\left(\bar{v} + N_v\frac{d\bar{v}}{dN_v}\right).$$

Comparing this with eq. (4.7), one obtains

$$V = \bar{v} + N_v\frac{d\bar{v}}{dN_v}. \tag{4.8}$$

Substituting eq. (4.6) for $dN_v/dt$ and eq. (4.8) for $V$ into eq. (4.7), one obtains:

$$\frac{df}{dt} = \left[n_i + f\left(p - \frac{1}{\bar{v}}\right)\right](1-f)\nu \exp\left(-\frac{\Delta W_a}{RT}\right)\left(\bar{v} + N_v\frac{d\bar{v}}{dN_v}\right). \tag{4.9}$$

In this equation $\bar{v}$ is known as a function of '$f$' determined from metallographic measurements; using Fullman's[50] equation,

$$\bar{v} = \frac{\pi^2 f}{8\bar{E}\,N_A}, \tag{4.10}$$

where $\bar{E}$ is the mean reciprocal of martensite plate lengths as intersected by a random plane,

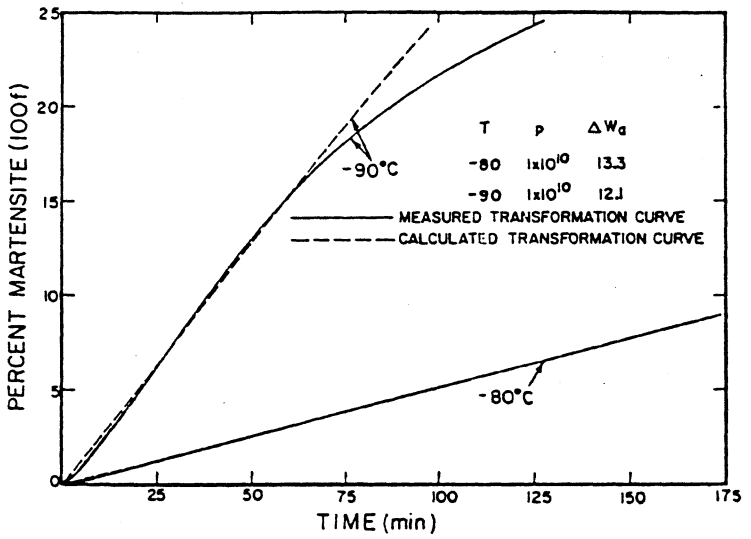


FIG. 11. Isothermal transformation curves obtained experimentally and by computation at −80 and −90°C (Fig. 2 in Ref. 36).

and $N_A$ is the number of martensite plates per unit area of random section. $N_v$ can be obtained as a function of '$f$' through eq. (4.4). The derivative $d\bar{v}/dN_v$ can also be evaluated leaving '$p$' and $\Delta W_\alpha$ as the only two adjustable unknown parameters. The results obtained by Pati and Cohen for the entire range of isothermal transformation in an Fe–24% Ni–3% Mn alloy are shown in Figs 11 and 12, and the experimental and calculated curves seem to agree well throughout the period of the transformation. It can also be seen from eq. (4.9) that if the autocatalytic factor $p > 1/\bar{v}$, the transformation rate increases with $f$. However, as the transformation progresses, $\bar{v}$ is significantly reduced so that $p < 1/\bar{v}$, and this leads to a decrease of the transformation rate with $f$. Pati and Cohen's model for isothermal transformation kinetics also explains the initial increase in the transformation rate followed by a final subsequent decrease.

The data from Fig. 12(a) show an interesting behavior. The transformation rate is maximum at −125°C, decreasing as the temperature is decreased to −140°C or increased to −115°C. By plotting these data in terms of isotransformation curves, one would obtain a C-type behavior characteristic of diffusional transformations. Fig. 13(a) shows as an illustration, isotransformation curves obtained by Shih *et al.*[26] for an Fe–23.2 pct Ni–3.62 pct Mn alloy. The nose (maximum transformation rate) temperature is ~ −140°C and the alloy definitely obeys a C-curve kinetics. The Raghavan–Pati–Cohen equations do not implicitly predict this response. They obey this behavior by calculating the activation energy from the temperature dependence of $df/dt$. As the temperature is decreased, the chemical driving force is increased. Hence, one should expect an increased rate. The only plausible explanations for the reduction of the rate at temperature below the nose is the motion of dislocations, which is thermally activated, is controlling nucleation of martensite. It is presently accepted that nucleation is controlled by thermally activated motion dislocations. There is, however, disagreement as to the identity of these dislocations. Olson and Cohen[55] espouse the earlier ideas of Magee and Paxton [cited in (16)] that the motion of interface dislocations through the lattice is the rate-controlling mechanism, while Kajiwara[42–44]

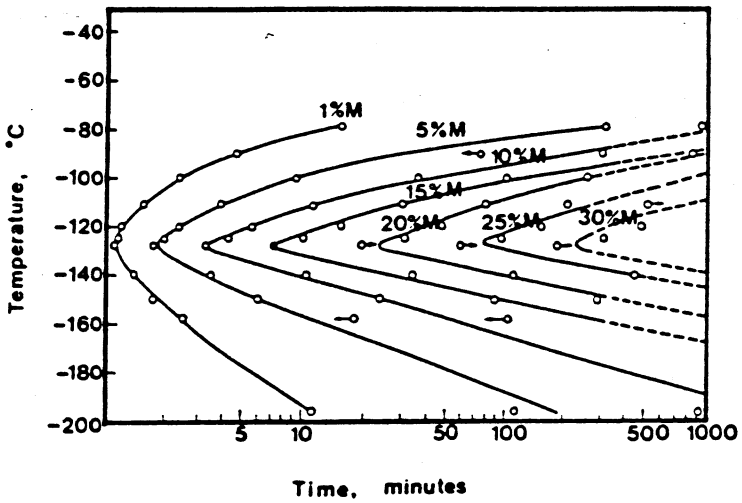


FIG. 13. (a) Isotransformation curves in time–temperature space for Fe–23.2 pct Ni–3.62 pct Mn alloy: martensite formed isothermally displays C-curve behavior (Fig. 2 in Ref. 26).

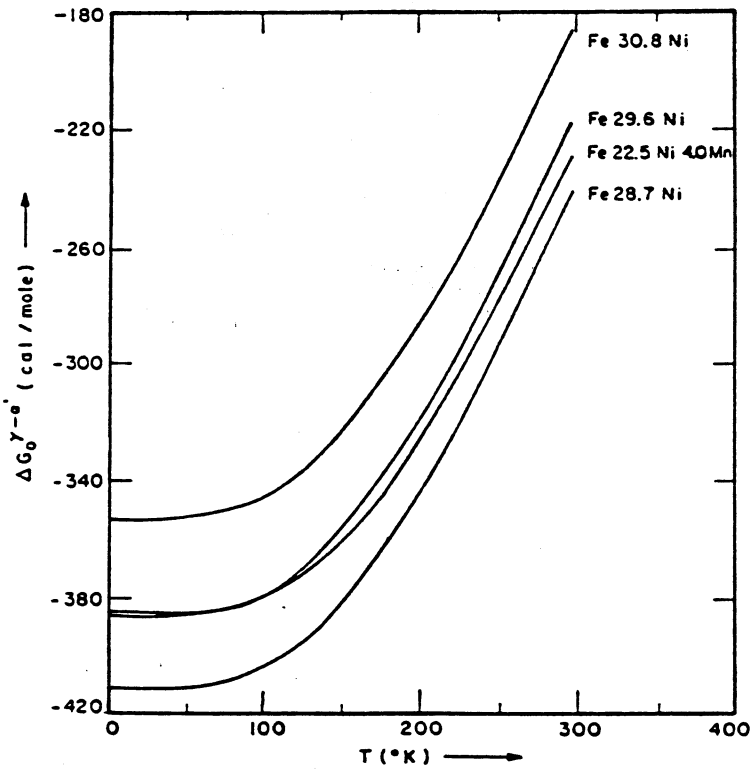


FIG. 13. (b) Chemical free-energy change for austenite–martensite transformation in four alloys (Fig. 5 in Ref. 38).

dislocations in overcoming these barriers. As the temperature is decreased, the stress required to overcome the short-range barriers increases, leading to a reduction in their mobility. At and below the nose temperature, the decrease in mobility of the dislocations overcomes the increase in driving energy leading to a reduction in the overall transformation rate.

The C-curve behavior can be explained thermodynamically if one assumes a linear relationship between the activation energy and the chemical driving energy. This seems to be an implicit assumption of the Kaufman–Cohen–Raghavan treatment. Kaufman and Cohen[60] briefly refer to the curvature in the chemical energy vs. temperature curve as a third-law-of thermodynamics effect [p. 185 of (60)]. Figure 13(b) shows that at temperatures below 150 K the curves show decreasing slope, tending to zero at 0 K. Olson and Cohen[65] later explain this behavior in a clearer fashion. The slope of the $\Delta G$ vs. $T$ curve is equal to:

$$\frac{\mathrm{d}\Delta G}{\mathrm{d}T} = \Delta S. \tag{4.10}$$

The third law of thermodynamics states that the entropy of pure substance is zero at 0 K. Referring to eq. (4.9) and assuming to a first approximation, that all terms are temperature-independent:

$$\frac{\mathrm{d}f}{\mathrm{d}t} = k \exp\left(\frac{\Delta W_a}{RT}\right) = k \exp\left(\frac{-A + B\Delta G}{RT}\right). \tag{4.11}$$

The temperature dependence of $\Delta G$ can be approximated by a quadratic fit:

$$\Delta G = C + DT + ET^2. \tag{4.12}$$

The maximum transformation rate $\dot{f}$ occurs at the nose of the C-curve and corresponds to $\mathrm{d}\dot{f}/\mathrm{d}T = 0$. Hence; the maxima of $\dot{f}$ occur at the temperatures:

$$T = \frac{D}{2E} \tag{4.13}$$

$$T = \frac{BD + \sqrt{(BD^2 - 4BE(A + BC)}}{2BE} \tag{4.14}$$

### 4.2. *Comparison of the Proposed Models*

The use of the partitioning formula by Raghavan and Entwisle[15] implies that the embryos are uniformly distributed within the material at all times during the transformation. This is only valid for two situations:

(i) prior to the start of the transformation, with only the preexisting embryos in the parent austenite; and
(ii) after substantial transformation ($> 10\%$) with martensite plates in most of the austenite grains.

The autocatalytic embryos are generally located in the immediate vicinity of the previously formed plates where there are significant strain fields. Hence, the volume immediately surrounding a martensite plate has a higher concentration of embryos than the volume away. This is also consistent with experimental observations. As such, with a non-uniform distribution of martensite plates, the partitioning formula of Fisher *et al.*[3] used by Raghavan

and Entwisle in their kinetic model is not an accurate description of the volume fraction transformed per nucleation event.

Thus the time sequence of plate formation has to be considered in computing isothermal transformation curves and parameters relating to the nucleation process. This was done by Raghavan[49] who adopted a different scheme for the partitioning effect in this model. However, it is still not clear whether modifications of this type will eventually achieve a satisfactory agreement or whether a more rigorous approach is required. Nor is there any experimental evidence available presently to support this formulation. Direct simulation of existing embryos by the stress fields of growing plates may also play an important part in increasing the total amount of transformation. Another factor which may be of importance as the transformation progresses is the effect of stress and strain fields of existing plates. A stage is eventually reached when all the remaining austenite is influenced by the neighbouring plates. These factors are also not incorporated in the proposed models based on the partitioning effect.

The model by Pati and Cohen[36] seems to be the most accurate as seen from the excellent agreement between experimental and calculated curves. This formulation has an advantage over the other two theories that it does not assume any particular model for the geometry of partitioning of the austenite by martensite plates. Quantitative metallographic measurements yield $\bar{v}$, the mean volume of a martensite plate. Based on this information, the martensitic transformation curves can be obtained with much greater accuracy. However, in this formulation $\bar{v}$ is not the mean volume per martensitic plate forming at any instant during the isothermal transformation, but rather the mean volume of all the plates present at any time; and hence can only be determined by direct measurements.

### 4.3 *Shortcomings of the Proposed Models*

In the computations of the isothermal transformation curves and the activations energies, $n_i$, which is the number of preexisting nucleation sites and $\nu$, the nucleation attempt-frequency, have been assigned different values by different investigators. Shih *et al.*[26] assumed $n_i$ to be $10^5$ per cm$^3$ for an austenite grain size of 0.18–0.25 mm, whereas Raghavan and Entwisle[15] considered $n_i$ to be $10^7$ per cm$^3$ for the grain sizes of the order of 0.05 mm. The most widely used estimate for the nucleation attempt frequency, $\nu$, is $10^{13}$ s$^{-1}$. However, values of $10^{14}$ and $10^{11}$ have also been considered by different authors.[17,29]

Apart from these still controversial issues the proposed kinetic models contain several troublesome facts:

(a) The total number of nucleation sites taking part in the transformation, given by the first term on the right hand side of eq. (4.1) does not consider the sites that are swept out in the volume of the transformed material.
(b) The use of a single activation energy to describe both the initial and autocatalytic nucleation.
(c) The consideration of an autocatalytic embryo as a separate entity from the parent phase.
(d) The dynamic propagation stress field is significantly different from the static stress field surrounding a martensite plate.

#### 4.3.1. *Total number of nucleation sites*

In the early stages of the transformation the "sweeping-out" effect is negligible. However, in the later stages of the transformation the "sweeping-out" term becomes dominant because

of the larger concentration of embryos. Gupta and Raghavan[51,52] attempted to compute the variation of the number of nucleation sites $n_t$ for martensite in a volume $V_0$ of the alloy as a function of the volume fraction being transformed. They proposed two limiting cases, when the sweeping-out effect is either negligible or dominant. If $v$ is the average volume of a martensite plate that forms between a martensite reaction $f$ and $f+\Delta f$, $V$ is the average volume of the austenite per nucleation site, at $f$ and $\Delta N$ plates form for $f$ fraction of martensite, then the number of nucleation sites $n_t$ for the condition $v \ll V$ (negligible sweeping-out effect) is given by

$$n_t = n_i + pf - N \tag{4.15}$$

and the condition $v \gg V$ (dominant sweeping-out effect),

$$n_t = [n_i - p\ell n(1-f)](1-f). \tag{4.16}$$

For the general case, they then adopted the probabilistic approach to determine the number of sites that are enclosed in each plate of average volume '$v$' subject to the constraint that at least one site was enclosed in this volume from which the plate was grown. Accordingly, they suggested that the total number of nucleation sites can be given by[51]

$$n_t = n_i + p\Delta f - \frac{n_t \Delta f}{(1-f)[1-\{1-v/(1-f)\}^{n_t}]} \tag{4.17}$$

where the different terms have their usual meanings. Knowing the empirical relationship between $v$ and $f$, one can determine $n_t$ by numerical integration of eq. (4.17).

Guimarães[53] criticized Gupta and Raghavan for overlooking several factors in their derivation. They considered that at any instant (fraction transformed), every available site, either preexisting or autocatalytically produced, had the same individual probability to end up inside a growing plate. Contrary to this, Guimarães suggested that the nuclei that are activated and originate the martensite plate are necessarily consumed, without choice. Only the remaining ones, critical or uncritical, but not activated, have the probability of ending up inside the martensite plates. As such, the nuclei that are activated cannot be introduced in the probability equation for the number of sites swept out.

Furthermore, Guimarães pointed out that the newly created sites due to autocatalysis are represented by the term $p\Delta f$ by Gupta and Raghavan in eq. (4.17). However, of the embryos or sites that are produced by autocatalysis, some fall in the martensite plates and can be termed "ghost sites". These ghost sites do not need to be accounted for in the equation for the number of sites being swept out. Hence, only the embryos produced by autocatalysis and lying in the austenite region have to be considered. Guimarães added that the $p\Delta f$ term should therefore be multiplied by a factor $(1-f)$. Gupta and Raghavan replied to this by stating that it was a question of how the autocatalytic sites were defined. They considered them to pertain to stress–strain centers generated by a martensite plate in the adjoining austenite. However if the autocatalytic sites are considered to pertain to all strain centers generated by a martensite plate (including those falling within the martensitic plates) then Guimarães' suggestions appear appropriate. The issue still remains questionable.

### 4.3.2. *Variation of activation energy*

The question of the distribution of activation energies during the course of transformation, and that of the distinction between autocatalytic and preexisting nucleation sites, was resolved by the small particle experiments of Cech and Turnbull[28] and Magee.[29] The experiments performed by Cech and Turnbull[28] will be discussed in Section 5. The present section deals

with the experiments performed by Magee[29] to determine the relative effectiveness of the various transformation sites and the nature of their distribution. Magee[29] also developed a technique to measure the nucleation rates in alloys where the bulk kinetics are so dominated by autocatalysis that meaningful isothermal measurements have previously not been obtained. He performed experiments on an Fe–24% Ni–3.65% Mn alloy powder, which shows completely isothermal kinetics in the bulk, and on Fe–22% Ni–0.49% C alloy powder which transforms by bursting. The results of his experiments are illustrated in the plots of Fig. 14. The variation in his particle fraction transformed with time is shown at different temperatures and for different particle diameters in the two alloys. For the Fe–24.2% Ni–3.65 Mn alloy, the effect of particle size is evident in Fig. 14(c): the larger particle size results in greater transformation. Figure 14(b) shows the C-curve behavior with more rapid transformation around 133 K. For the Fe–22% Ni–0.49% C alloy, the isothermal nature of the transformation can be observed in Fig. 14(c).

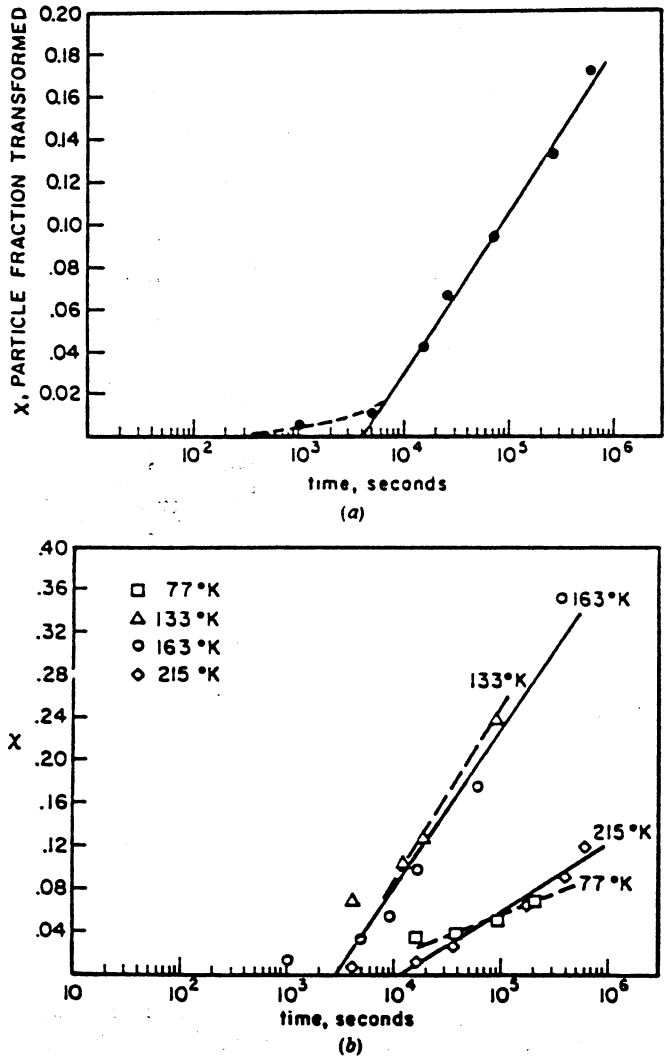


FIG. 14 (a–b).

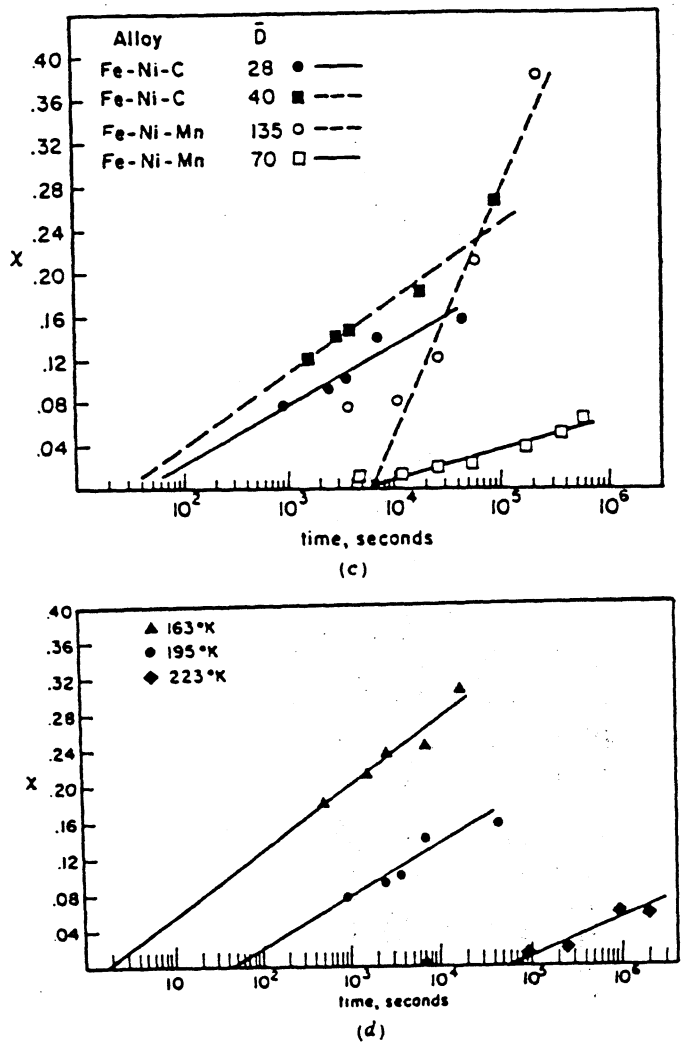


FIG. 14. Variation of particle fraction transformed, $\chi$, with time. (a) Fe–24.2% Ni–3.6% Mn at 195 K —98 $\mu$m particles; (b) Fe–24.2% Ni–3.6% Mn—98 $\mu$m particles at various temperatures; (c) Fe–24.2% Ni–3.6% Mn and Fe–22% Ni–0.4% C at two particle sizes, all samples reacted at 195 K; (d) Fe–22% Ni–0.49% C—28 $\mu$m particles at three reaction temperatures. (Fig. 11(a), (b), (c), (d) in Ref. 29.)

Magee proposed a model for isothermal martensitic kinetics from nucleation sites having a distribution of activation energies. He suggested that in this case the nucleation rate can be given by:

$$\frac{dN_v}{dt} = \int_0^\infty \nu \exp(-Q/RT) n^*(Q)\, dQ \tag{4.18}$$

where $n^*(Q)dQ$ is the number of nucleation sites per unit volume ($\chi^*/V_p$) having activation energies between $Q$ and $Q + dQ$. $\chi$ and $V_p$ are the particle fraction transformed and particle volume respectively. Considering $n^*(Q)$ constant above $Q_{min}$ [$= n^{*\prime}(Q)$], and equal to zero

below $Q_{min}$, eq. (4.18) can be integrated to give the nucleation rate at any time. Hence,

$$\frac{dN_v}{dt} = n^{*\prime}(Q)RT\nu \exp(-Q_{min}/RT). \tag{4.19}$$

Comparing this with the kinetic model by Pati and Cohen[36] [eg. (4.6)] it can be seen that the two equations are of the same form with (since $f = 0$):

$$n_i = n^{*\prime}(Q)\, RT \tag{4.20}$$

and

$$\Delta W_a = Q_{min}. \tag{4.21}$$

This implies that the previously calculated activation energies are the minimum energies in the distribution at the time of measurement. Furthermore, according to Magee,[29] the lower estimates of $n_i$ ($10^5\,cm^{-3}$) appear to be more reasonable in analyzing bulk isothermal kinetics. Hence, Magee's technique clearly allows for the measurements of reaction rate due solely to the sites present initially which makes it possible to show that the nucleation sites have a distribution of effectiveness.

## 5. Small Particle Experiments

The question of the nature of martensite nucleation, whether homogeneous of heterogeneous, was first resolved by the classic small particle experiments of Cech and Turnbull,[28] in 1956. It was believed that statistical composition fluctuations giving rise to localized regions of varying size and composition served as nucleation centers for martensite. These small regions occurred at high temperatures and were "frozen-in" on quenching. With a progressive decrease in temperature they became "supercritical", one after another, resulting in temperature dependent or athermal martensite transformation. In Fe–Ni alloys, the nucleation was predicted to occur as time-dependent and having the functional relationship to give a C-curve nucleation frequency vs. temperature. In these alloys the nucleation of martensite was catalysed by structural heterogeneities (strained regions) and the catalytic potency of these inhomogeneities was somewhat variable. There was evidence indicating that both, compositional as well as structural inhomogeneities, played an important role in the nucleation of martensite.

With the small particle experiments it was possible to determine the effectiveness of the various transformation sites and the nature of their distribution. It is particularly difficult to assess the actual number of active nucleation sites because their number is constantly changing due to the potent autocatalysis accompanying the transformation. Hence, with the small particle experiments it was possible to determine the nucleation rate from the initial sites alone and thereby reduce the levels of assumptions required in evaluating the activation energy, $\Delta W_a$.

Cech and Turnbull[28] performed experiments on Fe–30.2% Ni powder and observed that there were three possible martensite distribution configurations, as illustrated in Fig. 15. Their results showing the amount of martensite present after quenching the powder specimens at different temperatures are illustrated in Fig. 16. It was found that the percentage of martensite in a powder specimen was a function of the particle size, with smaller particles having a lesser extent of transformation than larger size particles. Figure 17 shows the plot of the relative fraction of particles containing martensite as a function of the particle size, at different temperatures. The fraction of particles nucleated increases with particle volume at any given

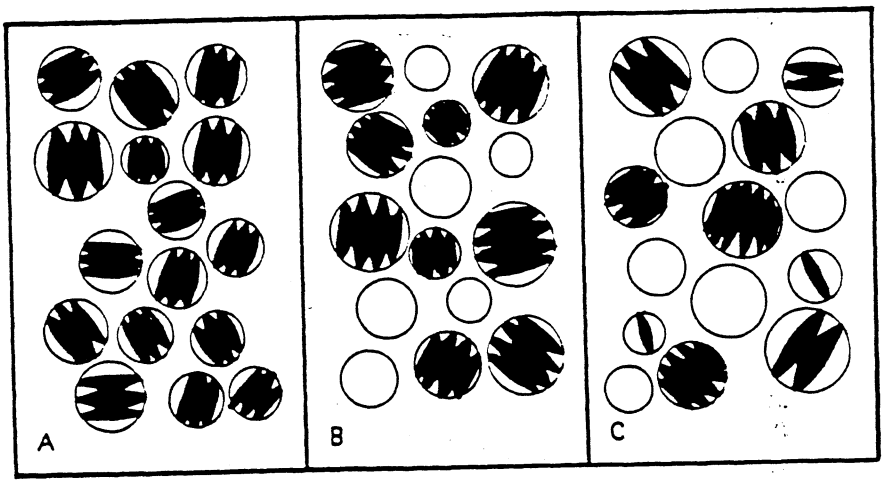


FIG. 15. Schematic of the three possible martensite distribution arrangements in powders. (A) Uniform degree of transformations in all particles. (B) Uniform degree of transformation in some particles and no transformation in others. (C) Varying degrees of transformation in some particles with no transformation in others (Fig. 5 in Ref. 28).

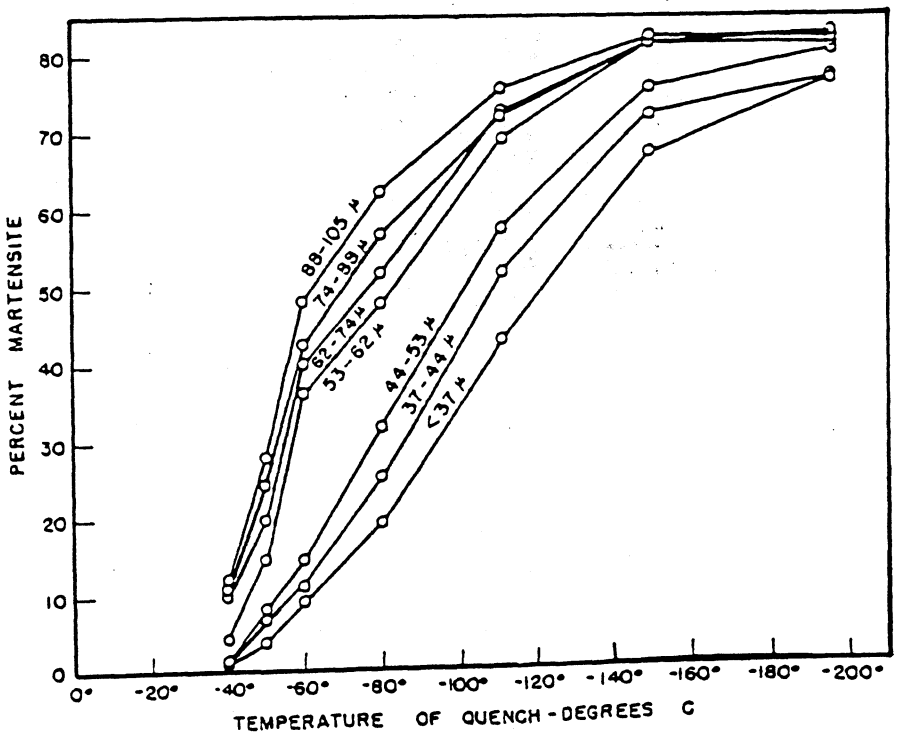


FIG. 16. Plot of the amount of martensite present after quenching as a function of temperature for different particles sizes (Fig. 4 in Ref. 28).

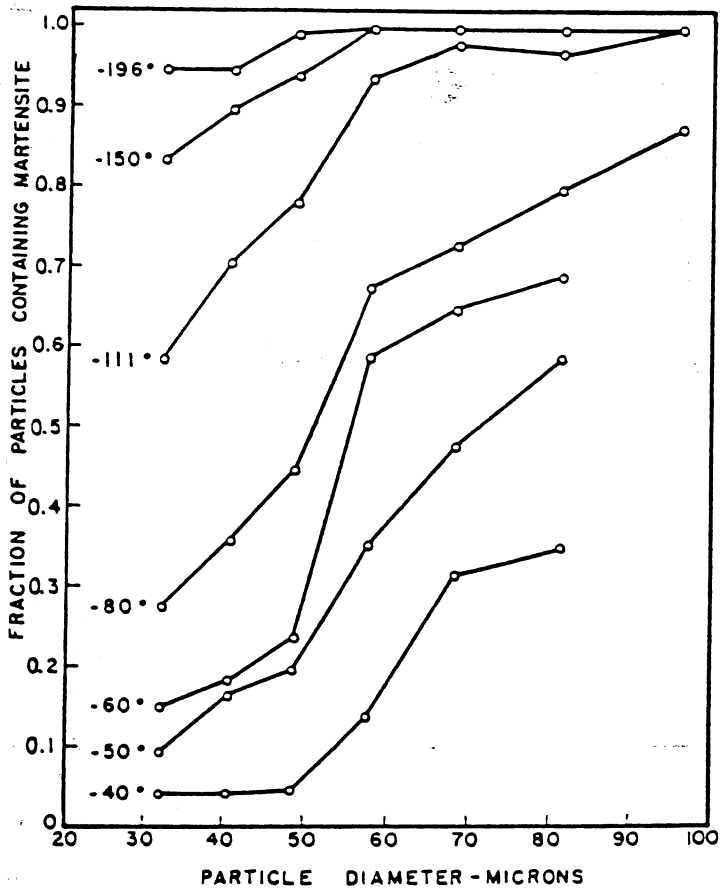


FIG. 17. Plot of the relative fraction of particles containing martensite as a function of the particle size at different temperatures (Fig. 8 in Ref. 28).

temperature. This indicates that the probability of finding a preexisting nucleation site in a small particle increases with the size of the particle, which is in support of the heterogeneous nature of martensite nucleation. Furthermore, for a given particle size, the fraction of particles where martensite nucleated increases with decreasing temperature of undercooling. This implies that weaker particles require more driving force, and hence, lower temperatures to become operative. In fact some particles may not transform at all even on cooling to temperatures approaching absolute zero. This signifies that the preexisting nucleation sites have a range of potencies, some requiring less and others more driving force.

Martensitic transformations are often autocatalytic because of the elastic stresses and plastic strains arising from the shape change. Such autocatalysis can spread throughout the volume of a bulk specimen and thus hinder the potential participation of less potent preexisting sites. However, in small particles, autocatalytic effects within a given grain are not transmitted to other particles and so the preliminary nucleation events in each particle must depend on its own preexisting sites only. Recently developed techniques like monitoring acoustic emission signals associated with bursting, can also be used to separate the effect of autocatalysis and thus be able to measure nucleation rates from initial sites alone.

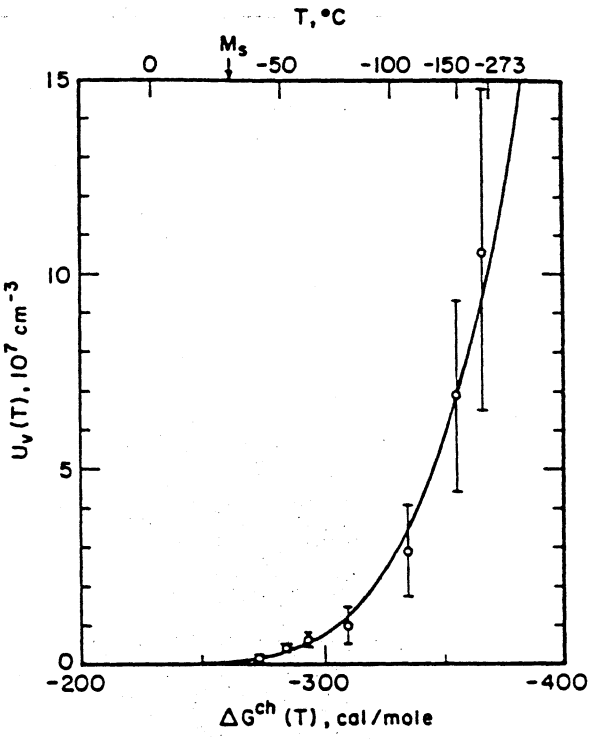


FIG. 18. Calculated (full line) and measured concentration of most potent nuclei as a function of temperature (Fig. 45 in Ref. 55).

Knorovsky[54] established the thermodynamic driving force necessary for the nucleation of martensite in single crystals and found that the driving force for autocatalytic nucleation was 200 J/mole lower than that for isolated nucleation at $M_s$ temperature.

Olson and Cohen[55] recently took Cech and Turnbull's[28] experimental data and determined the number of nucleation sites per unit volume, as a function of temperature. This was done assuming a critical driving force for the operation of these nuclei, composed of the well-known Olson–Cohen dissociated dislocation arrays. At $M_s$, the number of most potent nuclei is $10^6 cm^{-3}$ (one per 100 $\mu$m grain). As temperature is decreased, this number increases exponentially. Figure 18 shows that calculated curve, which correlates well with Cech and Turnbull's results (shown by bars).

## 6. GRAIN SIZE EFFECT ON MARTENSITE KINETICS

Raghavan and Entwisle[15] showed that the isothermal transformation curves (Fig. 2) are very sensitive to the grain size. The rate of isothermal transformation increases with the austenitic grain size, even when the final austenitizing temperature is held constant.

The autocatalytic parameter '$p$' is independent of the grain size. However, '$\bar{v}$', the mean martensitic plate volume, at any stage of the transformation $f$, is larger, the larger the grain size, which is true if the plates extend entirely across the austenitic grains or not. The factor $(p - 1/\bar{v})$ in eq. (4.9) controls the observed acceleration of the transformation due to

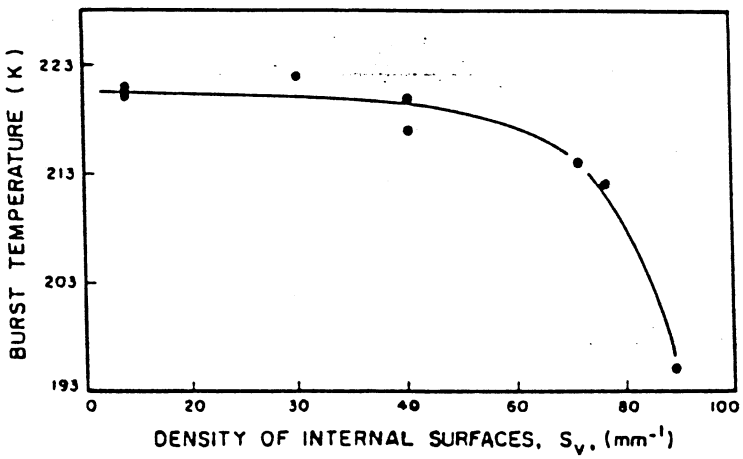


FIG. 19. Variation of burst temperature, $M_B$, with the density of internal surfaces (Fig. 2 in Ref. 56).

autocatalysis. Hence, under such conditions the autocatalytic effect ($p - 1/\bar{v}$) is greater when the grain size is larger.

Guimarães and Gomes[56] also observed that a change in grain size affected the burst temperature as well as its kinetics. Figure 19 shows the variation of the burst temperature, $M_B$, with the density of the internal surfaces, $S_v$, consistent with the observations of Umemoto and Owen.[57] For large grain sizes (small $S_v$) the temperature dependence of $M_s$ is not very large; for smaller grain sizes (larger values of $S_v$), there is a substantial drop in $M_s$. Figure 20 illustrates the variation of martensite volume fraction transformed in a burst, $V_v$, and the fraction of material in grains partially transformed, $G_g$, as a function of $S_v$. Essentially, the amount of martensite formed in a burst decreases with increasing $S_v$.

Thus the relative importance of the processes of the propagation and "filling-in" during the burst is determined by the austenite grain size. Coarse-grained austenite is associated with

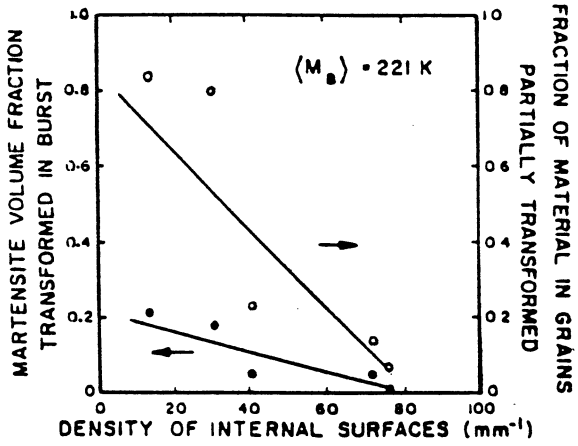


FIG. 20. Variation of martensite fraction transformed in a burst and the burst of material in grains partially transformed as a function of the density of internal surface (Fig. 4 in Ref. 56).

ess-heterogeneous burst transformation. This can be explained by the fact that the propagation of a burst requires martensite nucleation in many adjacent grains which are stimulated by the elastic–stress fields of the plates in the neighborhood. The intensity of the field set up by a plate is proportional to its size which is limited by the grain size of the austenite. Again the formation of one plate in a coarser grain causes a longer range perturbation (per unit volume of the material). Since there are less grains per unit volume in coarse grained materials the corresponding burst will be longer and spread more. Guimarães and Gomes[56] also determined that the rate of propagation of martensite was proportional to the square of the volume fraction of the material in the partially transformed grains; and reduction of the austenite grain size resulted in a highly heterogeneous transformation and small burst. This suggests that grain size has an important influence on the role of grain-to-grain "spreading" and intragranular "filling-in" modes of autocatalysis.

## 7. Activation Energy Dependence on Driving Force and Kaufman–Cohen Model

Shih *et al.*[26] estimated the activation energy for martensite plates forming at the beginning of the transformation using only the most potent of the preexisting embryos. Assuming a constant rate of nucleation up to the first detectable amount of martensite (0.2%), they calculated the activation energies from the following equations[26]:

$$N = n_i v \exp(-\Delta W_a/RT) \tag{7.1}$$

and

$$Nv_i\tau_i = 0.002, \tag{7.2}$$

where $v_i$ is the volume of the first plates to form and $\tau_i$ is the time to produce 0.2% martensite. Considering $n_i = 10^3$ cm$^{-3}$, they computed the activation energies to be in the range of 25,000–60,000 J/mole for temperatures between $-196$°C to $-90$°C in Fe–Ni–Mn and Fe–Mn–C alloys.

Pati and Cohen[27] employed quantitative metallography for direct measurements of $\bar{v}$ and also accounted for the increase in the nucleation rate due to autocatalysis. Taking $n_i = 10^7$ cm$^3$ for Fe–24% Ni–31% Mn alloys they showed that the activation energies lie between 25,000–65,000 J/mole and decrease monotonically with decreasing reaction temperature from $-70$°C to $-196$°C.

The activation energies for isothermal martensite nucleation in Fe–Ni–Mn alloys show a linear dependence on the chemical driving force (which on its turn is dependent on the temperature) of the transformation as shown in Fig. 21 and obey the empirical relationship:

$$\Delta W_a = 1.05 \times 10^{-28}(\Delta G) + 3.66 \times 10^{-19} \text{ J/event.} \tag{7.3}$$

For an Fe–29.2% Ni alloy (lenticular morphology) the relationship is:

$$\Delta W_a = 3.69 \times 10^{-28}(\Delta G) + 8.27 \times 10^{-19}. \tag{7.4}$$

These linear relationships are consistent with the Kaufman–Cohen model for an oblate-spheroidal embryo for isothermal nucleation.

Kaufman and Cohen[59,60] considered the embryo to be an oblate spheroid of martensite with an array of screw dislocation loops in the interface. This model is an extension of Knapp and Dehlinger's[58] original ideas on the embryo. The Kaufman–Cohen model is dependent on the occurrence of a lattice-invariant deformation. Kinetic experiments on the coherent

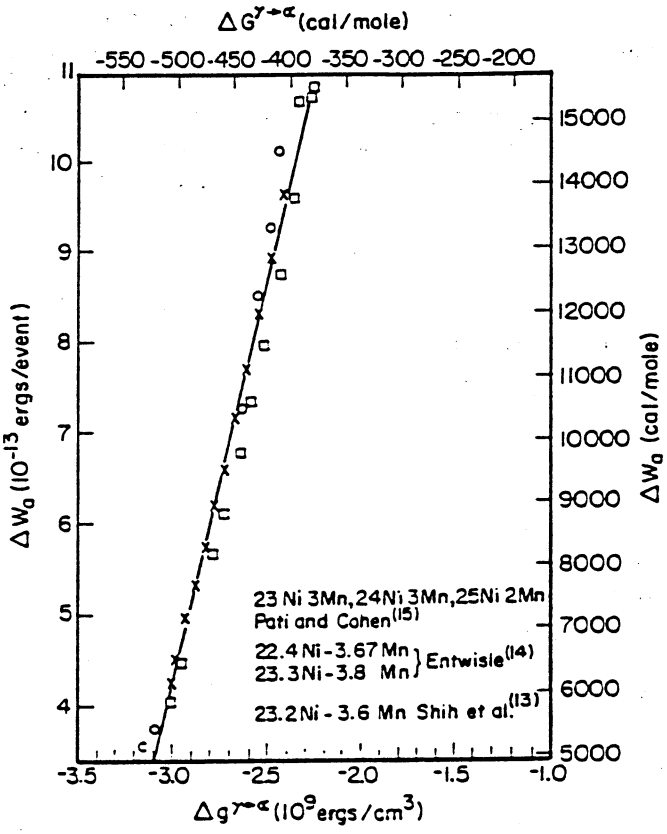


FIG. 21. Measured activation energies for the isothermal martensitic transformation in Fe–Ni–Mn alloys as a function of the free energy change accompanying the transformation (Fig. 4 in Ref. 27).

fcc-to-hcp martensitic transformation, where the lattice-invariant deformation is absent, give essentially the same linear dependence of the activation energy on the driving force. It has been recently established that the motion of interfacial dislocations even in the absence of a lattice-invariant deformation, can give rise to thermally activated behavior. Magee[16] was the first to suggest that the nucleation rate was controlled by dislocation motion. Olson and Cohen,[40] later applied this to coherency dislocation motion during nucleation by defect dissociation. For a process with a "stress-free" activation energy and a fixed activation volume, coherency dislocation motion under the influence of a negative fault energy gives a linear $\Delta W_a$ vs. $\Delta G$ relationship. It is believed,[55] that the $\Delta W_a$ vs. $\Delta G$ function possesses in fact some curvature, which is consistent with the behavior observed in slip. The linear relationship (Fig. 21) as is observed for Fe–Ni–Mn and Fe–Ni alloys, identifying an isothermal transformation represent different positions of a common $\Delta W_a$ vs. $\Delta G$ master curve. The high and low energy regions in this master curve have, so far, not been experimentally accessible.

The Kaufman–Cohen linear relationship assumes slip as the lattice invariant shear, whereas twinning is the operative mode in Fe–Ni–Mn and Fe–Ni alloys. In this model the driving stress on the interface has to overcome the restraining stress arising from the surface-energy and strain-energy terms, as well as provide for the athermal creation of new dislocation loops at the tips of the embryos.

The activation energy for the spreading of this interface is related to the driving force with the following relationship[17]:

$$\Delta W_a = 4 \times 10^{-2} \left(\frac{\sigma}{A}\right)^{1/2} \left[3\sigma r_e^{3/2} + \Delta G \left(\frac{\sigma}{A}\right)^{1/2} r_e^2\right] \text{(ergs/event)} \qquad (7.5)$$

where $\sigma$ is the interfacial energy in ergs/cm$^2$, $A$ is the strain-energy factor ($2.1 \times 10$ J/cm$^3$), and $r_e$ is the embryo radius in cm and also provides a measure of the "strength" of the most-potent nucleation sites. As shown by eqs (7.3) and (7.4) a straight line relationship is in fact observed between the experimentally determined activation energies and $\Delta G$ which changes with composition and temperature. The slope and intercept of the line in Fig. 21 lead to the values of $r_e$ and $\sigma$. For Fe–Ni alloys these are computed to be 420 Å and $110 \times 10^{-7}$ J/cm$^2$ respectively and for Fe–Ni–Mn alloys $r_e$ and $\sigma$ are 220 Å and $120 \times 10^{-7}$ J/cm$^2$.

Since $r_e$ represents the potency of the embryo rather than the actual size, it can be seen that Mn reduces the embryo potency when added to Fe–Ni alloys. With increasing embryo potency for the martensitic transformation, the nucleation kinetics changes over from essentially isothermal C-curve kinetics in Fe–Ni–Mn alloys to athermal behavior in Fe–Ni alloys.

Pati and Cohen[27] showed that if the most potent embryos are smaller than 210 Å, there is virtually complete isothermal C-curve kinetics observed. For embryo sizes greater than 225 Å the curves lose their shape and tend to become horizontal leading to truly athermal kinetics. This effect is illustrated in Fig. 22, which is a plot of time for 0.2% transformation as a function of reaction temperature for different embryo radii in Fe–24% Ni–3% Mn alloy.

## 8. Kinetics of Mechanically-Induced Martensite

The fourth group in the classification presented in Fig. 1, mechanically-induced martensite, is described next. It is well known that both applied stress and strain affect the martensitic transformation. Hence, mechanically-induced martensite has been classified into stress

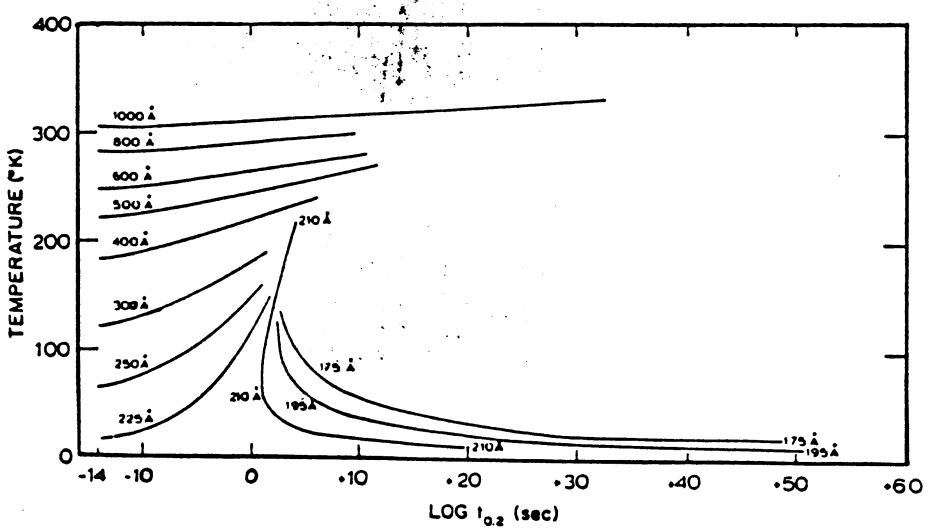


FIG. 22. Plot of calculated time for 0.2% transformation as a function of reaction temperature for indicated embryo radii in Fe–24% Ni–3% Mn alloy, having a grain size of 0.025 mm (Fig. 6 in Ref. 27).

assisted martensite and strain-induced martensite. In stress-assisted martensite the applied stress interacts directly with the strains generated by the martensitic transformation (shear and dilatational). The theoretical treatment is given by Patel and Cohen.[61] The product of the stress and strain gives a mechanical work term which either helps or hinders the transformation. Stress assisted martensite usually forms below the yield stress of the material. At stresses that produce substantial plastic strains, new nuclei are formed by plastic deformation. Martensite formed at these new nuclei is called strain-induced martensite.

Olson and Cohen[62] studied the kinetics of strain-induced martensite transformation in AISI 304 stainless steel. They developed a model for the formation and operation of nuclei as a function of plastic strain and compared their predictions successfully with experimental results obtained by Angel.[63] In AISI 304 stainless steel plastic deformation produces shear bands, twin bands, and packets of stacking faults and $\epsilon$ martensite. The intersection of these planar features is the favored nucleation site for martensitic transformation. Olson and Cohen proposed equations for the shear band density and their intersections and arrived at the equation:

$$f = 1 - \exp\left\{-\frac{\bar{v}(\alpha')K}{(\bar{v}(sb)^n} P_r[1 - \exp(-\alpha\varepsilon)]^n\right\} \tag{8.1}$$

where $v(\alpha')$ is the average volume per martensitic unit, $\bar{v}(sb)$ is the average volume of a shear band, $K = \pi d^2/16$ ($d$ is the average austenitic grain size), $P_r$ is the probability that an intersection will form an embryo, $n$ is related to the number of intersections, $\alpha$ is a strain-independent constant, and $\varepsilon$ is the plastic strain. As expected with such a generous number of parameters, they found an excellent fit, shown in Fig. 23. It is significant to observe that the curves have the same sigmoidal shape as a function of time and that the saturation value of the transformation increases with decreasing temperatures.

Guimarães[64] proposed an alternative formulation, leading to the equation:

$$\ell n \frac{R+f}{R(1-f)} = Z(R+1)\epsilon \tag{8.2}$$

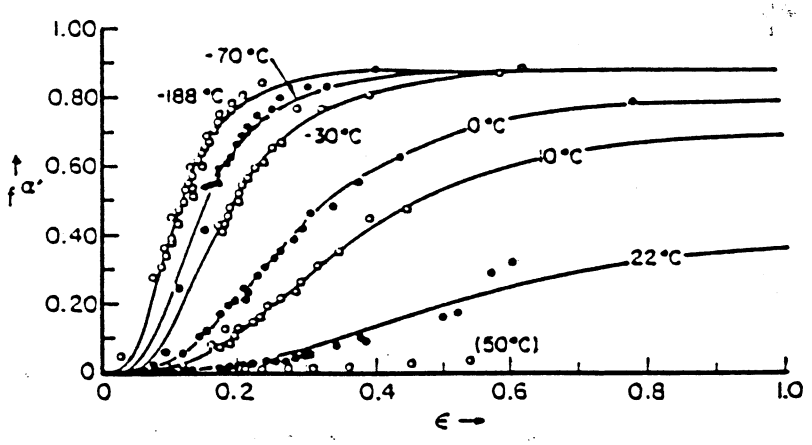


FIG. 23. Comparison of calculated transformation curves with data of Angel[63] for a 304 stainless steel. Experimental data are indicated by points. The solid curves represent the best fit of the derived expression for each temperature, consistent with the assumed temperature dependence of the $\alpha$ and $\beta$ parameters (Fig. 1 in Ref. 62).

$R$ is equal to the ratio $n_i^0/p$ between the initial nucleation sites and the autocatalytic factor, $Z$ is a parameter related to the probability of nucleation and to the average volume of the martensite plates. This model was tested against experimental data for high and low stacking fault energy alloys.[62,63]

Olson and Cohen[65] also applied the Pati–Cohen kinetics principles to the stress-assisted martensite, which governs the plastic flow behavior of TRIP steels in the low temperature regime. Olson and Azrin[66] had earlier established that the stress-assisted transformation was most operative at low temperatures, while at higher temperatures strain-induced transformation was important. The stress-assisted transformation has two effects: a "softening" mainly due to the shear of the martensite decreasing the applied shear stress; and a "hardening", due to the stronger phase inserted in the lattice, dislocations, etc. Olson and Azrin had found that, at low temperatures, the fraction transformed, $f$, was proportional to the plastic strain $\epsilon$. A constant strain leads therefore to a constant transformation rate, $\dot{f}$. They obtained the following equation to express the applied stress, as a function of the fraction transformed, $f$, for a constant transformation rate, $\dot{f}$:

$$\sigma(f) = -\left(B\frac{\partial \Delta\sigma}{\partial \sigma}\right)^{-1}\left[A + B\Delta G + RT\ell n\frac{\dot{f}}{(n_i + p\dot{f} - N_v)(1-f)Vv}\right]. \tag{8.3}$$

Here, A and B are constant parameters and can be determined from temperature dependence of chemical free energy ($\Delta G$). By substituting $\epsilon$ and $\dot{\epsilon}$ for $f$ and $\dot{f}$ (with experimentally determined proportionality factors) one arrives at the predicted $\sigma$–$\epsilon$ behavior, shown in Fig. 24, when plastic flow is controlled by stress-assisted isothermal martensitic transformation. The agreement between observed and calculated curves is good up to a strain of 0.04. The absence of work hardening, due to the softening effect of the martensite being formed as a function of strain, is clearly seen. This effect saturates at $-0.07$, when martensite transformation is complete.

The existence of martensite at a potential nucleation site involves three kinds of deformations: "lattice deformation" for generating a martensite lattice from austenite;

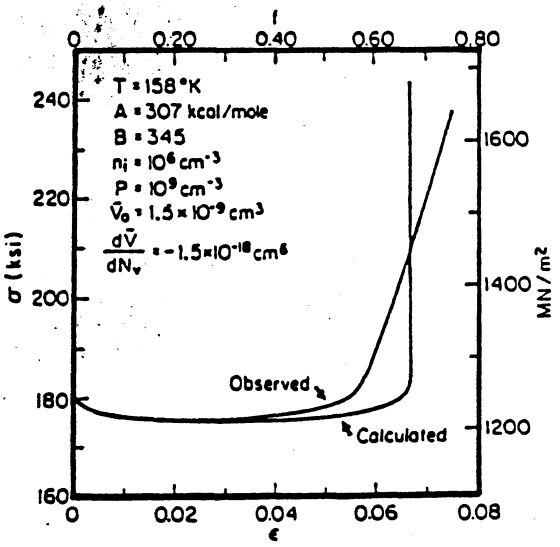


FIG. 24. Comparison between observed and calculated (by Olsen and Cohen[65]) stress–strain curves for TRIP steel (Fig. 6 in Ref. 65).

"lattice invariant deformation" for producing a strain-free interface between the two phases; and "plastic deformation in austenite" to account for the accommodation of shape strain of martensite. The kinetics of mechanically-induced martensite studied by Olson and Cohen[62,65] have been based on a model which considers the thermally activated motion of partial dislocations bounding the semi-coherent embryo to be the most probable rate limiting step.[40] Kajiwara[42–44] investigated the kinetic behavior of isothermal martensitic transformation under constant loads. He suggested that the drastic increase of transformation rate, above the yield stress of the austenite, cannot be explained by the usual approach that the work done by applied stress on the transforming martensite plate increases the driving force for the transformation. In contrast to this the applied stress helps the thermally activated movement of lattice dislocations in austenite and consequently makes possible the plastic accommodation of the shape strain of the nucleating martensite phase. Hence, according to Kajiwara[42–44] such dislocation motion in austenite is the actual rate-controlling step for isothermal martensite formation. However, Kajiwara[42–44] does not have quantitative evidence to support his model. Nevertheless, his experiments are very interesting and some of his results are reproduced in Fig. 25. Isothermal transformation at 77 K was monitored for an Fe–23 pct Ni–4 pct Mn alloy with a superimposed stress. The stress provided an additional driving force. Two grain sizes were used: 12 $\mu$m and 65 $\mu$m. The yield stresses at 77 K were found to be 255 and 220 MPa, respectively. For the 12 $\mu$m specimen, one observes a dramatic increase in $df/dt$ when the yield stress is exceeded. The same trend seems to be observed for the 65 $\mu$m specimen. While the effect of stress on the kinetics is to be expected and is consistent with Olson and Cohen's[65] work on stress-assisted martensite, the discontinuous increase when the yield stress is exceeded cannot be simply interpreted in terms of this

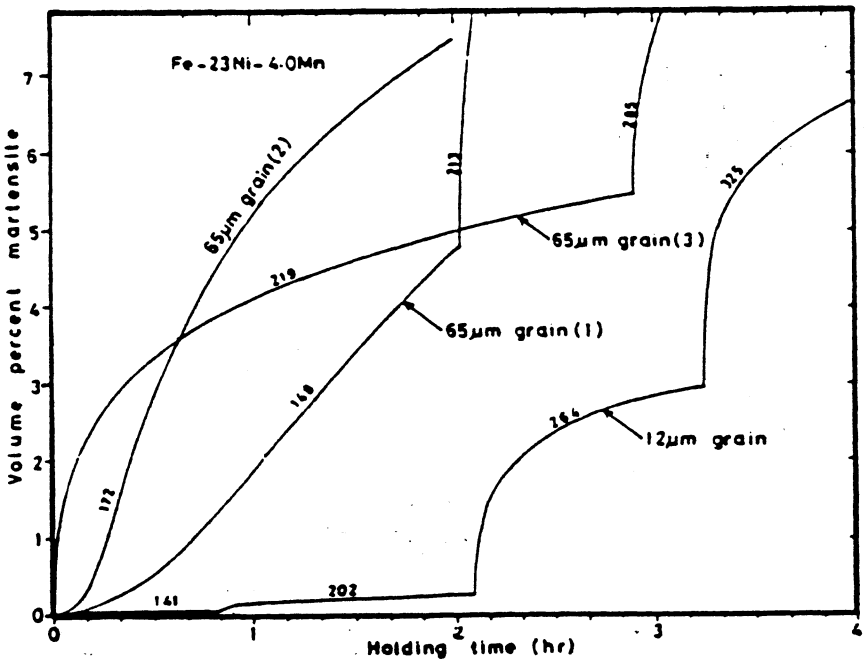


FIG. 25. Tranformation kinetics for Fe–23 pct Ni–4 pct Mn alloy of two grain sizes at 77 K under various levels of stress (stresses in MPa are marked on curves) (Fig. 1(a) in Ref. 43).

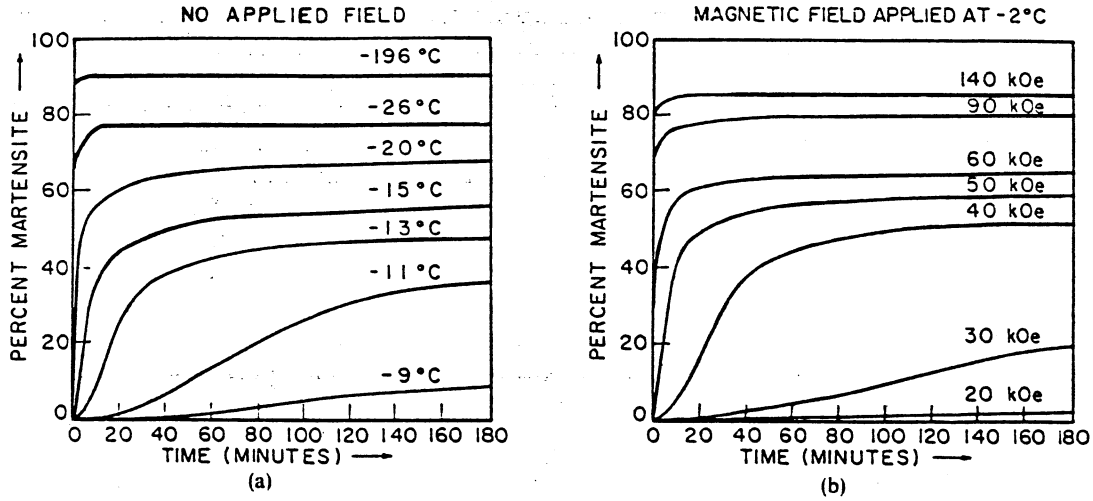


FIG. 26. (a) Transformation kinetics for Fe–29. 6 pct Ni alloy at varying temperatures (Fig. 9 in Ref. 38). (b) Transformation kinetics for same alloy at −2°C and varying levels of applied magnetic field (Fig. 10 in Ref. 38).

subjected a Fe–22.5% Ni–4% Mn alloy to magnetic field. This alloy did not exhibit any martensitic transformation under zero-field (transformation was so sluggish that it could not be observed). The magnetic field greatly accelerated the reaction rate, as can be seen in Fig. 27, where a C-curve behavior is observed, with the nose temperature at −120°C. This C-curve behavior is characteristic of this composition range (both Ni and Mn). It is due to the low autocatalytic factor and is explained in Section 4.2. Figure 12(b) shows an alloy with close composition, but which transforms in the absence of a magnetic field.

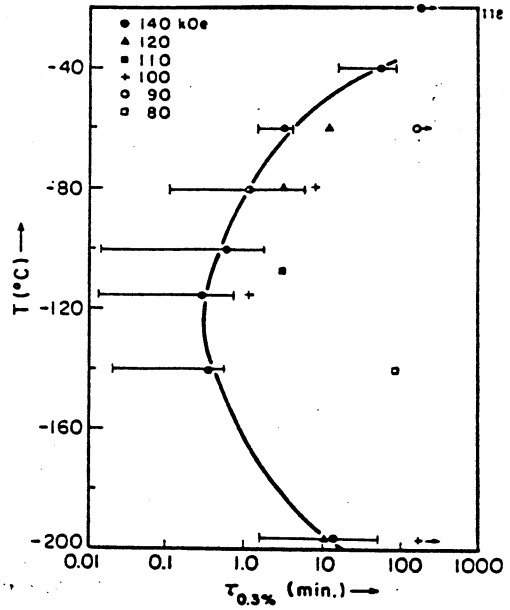


FIG. 27. Time to transformation to 0.3 pct martensite under a magnetic field of 140 KOe as a function of temperature for Fe–22.5 pct Ni–4 pct Mn alloy (Fig. 26 in Ref. 38).

(k) Mechanically-induced martensite is described from a kinetic point-of-view. The fraction transformed is expressed as a function of stress for stress-assisted martensite and as a function of strain for strain-induced martensite.

(l) It has been conclusively shown that externally-applied magnetic fields accelerate the rate of transformation, by providing an additional driving energy.

It can be concluded from the critical analysis of the work that the kinetics of martensitic transformation is fairly well understood. The Pati–Cohen equation describes fairly well the process; and the effects of composition, external stresses, and magnetic fields are understood and quantitatively described. On a more fundamental level, the tie-in with the mechanisms responsible for nucleation is not complete yet. While the earlier kinetic models used the Kaufman–Cohen–Raghavan concept of critical nucleus size in the interpretation of the activation energy and driving energy terms, the same kinetic equations can be linked to other models for nucleation. The latest attempt by Olson and Cohen seems to be fairly successful in establishing the rate controlling step for martensitic nucleation as being through the motion of the interfacial (martensite–austenite) dislocations. This linkup is carried out in a fairly indirect way; from the kinetics, the temperature dependence of the activation energy for nucleation is established. The chemical driving energy is calculated from thermodynamics. Thus, a relationship between chemical driving energy and activation energy is established. This leads directly to the determination of the activation volume for the movement of dislocation which establishes the rate controlling step. It should however be realized that the same kinetic data could be successfully used to provide fundamental parameters if other nucleation processes were postulated (or established).

## References


1. G. V. Kurdjumov and O. P. Maksimova, *Dokl. Akad, Nauk SSSR* **61** (1948) 83; **73** (1950) 95.
2. J. C. Fisher, J. H. Hollomon and D. Turnbull, *J. appl. Phys.* **19** (1948) 775.
3. J. C. Fisher, J. H. Hollomon and D. Turnbull, *Trans. AIME* **185** (1949) 691.
4. F. Forster and E. Scheil, *Ztsch. Metallkunde* **28** (1936) 295.
5. F. Forster and E. Scheil, *Naturwissenschaften* **25** (1937) 439.
6. F. Forster and E. Scheil, *Ztch. Metallkunde* **32** (1940) 165.
7. R. F. Bunshah and R. F. Mehl, *Trans. AIME* **197** (1953) 1251.
8. M. A. Meyers, *Met. Trans.* **10A** (1979) 1723.
9. G. Lormand, M. Robin and P. F. Gobin, *Metallogr.* **374** (1980) 369.
10. K. Takashima, Y. Higo and S. Nunomura, *Scripta Metall.* **14** (1980) 489.
11. J. M. Galligan and T. Garosshen, *Nature* **274** (1978) 674.
12. T. J. Garosshen and J. M. Galligan, *Scripta Metall.* **14** (1980) 1111.
13. B. I. Voronenko, *Met. Sc. and Heat Treat of Metals*, **24** (7–8) (1982) 545.
14. A. N. Moiseyev, L. I. Izyumova, M. P. Usikov and E. I. Estrin, *Physics Metals Metallogr.* **51** (4) (1981) 137–146.
15. V. Raghavan and A. R. Entwisle, Iron and Steel Inst. Special Report, No. 93, p. 30 (1965).
16. C. L. Magee, The nucleation of martensite, in *Phase Transformations*, ASM, Metals Park, Ohio, p. 115 (1970).
17. V. Raghavan and M. Cohen, *Met. Trans.* **2** (1971) 2409.
18. A. R. Entwisle, *Met. Trans.* **2** (1971) 2395.
19. J. R. C. Guimarães, *Rev. Lat. de Met. y Mat.* **1** (1981) 3.
20. B. L. Averbach and M. Cohen, *Trans. ASM* **41** (1949) 1024.
21. S. C. Das Gupta and B. S. Lement, *Trans. AIME* **191** (1951) 727.
22. E. S. Machlin and M. Cohen, *Trans. AIME* **191** (1951) 746.
23. E. S. Machlin and M. Cohen, *Trans. AIME* **194** (1952) 489.
24. S. A. Kulin and G. R. Speich, *Trans. AIME* **194** (1952) 258.
25. R. E. Cech and J. H. Hollomon, *Trans. AIME* **197** (1953) 685.
26. C. H. Shih, B. L. Averbach and M. Cohen, *Trans. AIME* **203** (1955) 183.
27. S. R. Pati and M. Cohen, *Acta Met.* **17** (1969) 189.

8. R. E. Cech and D. Turnbull, *Trans. AIME* **206** (1956) 183.
9. C. L. Magee, *Met. Trans.* **2** (1971) 2419.
0. T. Honna, *J. Japan Inst. Metals* **21** (1956) 127.
1. T. Philibert and C. Crussard, *J. Iron Steel Inst.* **180** (1955) 39.
2. J. Philibert, *I.R.S.I.D. Serie*, A139 (1956) 55.
3. J. Woodilla, P. G. Winchell and M. Cohen, *Trans. TMS-AIME* **215** (1959) 849.
4. R. B. G. Yeo, *Trans. AIME* **224** (1962) 1222.
5. A. V. Anandaswaroop and V. Raghavan, *Scripta Metall.* **3** (1969) 221.
6. S. R. Pati and M. Cohen, *Acta Metall.* **19** (1971) 1327.
7. A. R. Entwisle and J. A. Feeney, *The Mechanisms of Phase Transformations in Crystalline Solids*, Inst. of Metals Monograph, No. 33 (1969).
8. M. K. Korenko, Martensitic Transformations in High Magnetic Fields, D.Sc. Thesis, MIT, Cambridge, Massachusetts, (1973).
9. S. K. Gupta and V. Raghavan, *Acta Metall.* **23** (1975) 1239.
0. G. B. Olson and M. Cohen, *Met. Trans.* **7A** (1976) 1897; **7A** (1976) 1905; **7A** (1976) 1915.
1. V. I. Kolomytsev, V. A. Lobodyuk and G. I. Savvakin, *Phys. Metals* **3** (6) (1981) 1063.
2. S. Kajiwara, *Phil. Mag. A* **43** (1981) 1483.
3. S. Kajiwara, *J. Physiol.* Colloque C4 (1982) 97.
4. S. Kajiwara, *Acta Metall.* **32** (1984) 407.
5. D. Z. Yang and C. M. Wayman, *Metallog.* **17** (1984) 131.
6. C. A. V. de A. Rodrigues, C. Prioul and L. Hyspecka, *Met. Trans.* **15A** (1984) 2193.
7. N. N. Thadhani, An Investigation into Martensitic Transformation Induced by a Tensile Stress Pulse, Ph.D. Thesis, New Mexico Institute of Mining and Technology, Socorro, NM (1984).
8. N. N. Thadhani and M. A. Meyers, *Acta Metall.* accepted, in press (1985).
9. V. Raghavan, *Acta Metall.* **17** (1969) 1299.
0. R. L. Fullman, *Trans. AIME* **197** (1953) 447.
1. S. K. Gupta and V. Raghavan, *Scripta Metall.* **9** (1975) 917.
2. S. K. Gupta and V. Raghavan, *Scripta Metall.* **10** (1976) 787.
3. J. R. C. Guimarães, *Scripta Metall.* **10** (1976) 783.
4. G. A. Knorovsky, Autocatalysis of Martensitic Transformations, Sc.D. Thesis, Massachusetts Institute of Technology, Cambridge, MA (1977).
5. G. B. Olson and M. Cohen, Dislocation theory of martensitic transformations, in *Dislocations in Solids* (edited by F. R. N. Nabarro), North Holland Publishing Inc., to be published (1986).
6. J. R. C. Guimarães and J. C. Gomes, *Acta Metall.* **26** (1978) 1591.
7. M. Umemoto and W. S. Owen, *Met. Trans.* **5A** (1976) 783.
8. H. Knapp and U. Dehlinger, *Acta Metall.* **4** (1957) 289.
9. L. Kaufman and M. Cohen, *Trans. AIME* **206** (1956) 1393.
0. L. Kaufman and M. Cohen, *Prog. Met. Phys.* **7** (1958) 165.
1. J. R. Patel and M. Cohen, *Acta Metall.* **1** (1953) 531.
2. G. B. Olson and M. Cohen, *Met. Trans.* **6A** (1975) 791.
3. T. Angel, *J. Iron Steel Inst.* **77** (1954) 165.
4. J. R. C. Guimarães, *Trans. J.I.M.* **18** (1977) 803.
5. G. B. Olson and M. Cohen, *Met. Trans.* **13A** (1982) 1907.
6. G. B. Olson and M. Azrin, *Met. Trans.* **9A** (1978) 713.
7. Ye. A. Fokina, L. V. Smirnov and V. D. Sadovskiy, *Physics of Metals Metallogr.*, **19** (1965) 73.
8. E. I. Estrin, *Physics Metals Metallogr.* **19** (1965) 117.
9. P. A. Malinen and V. D. Sadovskiy, *Physics Metals Metallogr.* **21** (1960) 139.
0. P. A. Malinen, V. D. Sadovskiy and I. P. Sorokin, *Physics Metals Metallogr.* **24** (1967) 101.
1. C. T. Peters, P. Bolten and A. P. Miodownick, *Acta Metall.* **20** (1972) 881.